



HAL
open science

Adaptation to host in *Vibrio vulnificus* , a zoonotic pathogen that causes septicemia in fish and humans

Carla Hernández-cabanyero, Chung-te Lee, Verónica Tolosa-enguis, Eva Sanjuán, David Pajuelo, Felipe Reyes-lópez, Lluís Tort, Carmen Amaro

► **To cite this version:**

Carla Hernández-cabanyero, Chung-te Lee, Verónica Tolosa-enguis, Eva Sanjuán, David Pajuelo, et al.. Adaptation to host in *Vibrio vulnificus* , a zoonotic pathogen that causes septicemia in fish and humans. *Environmental Microbiology*, 2019, 21 (8), pp.3118-3139. 10.1111/1462-2920.14714 . hal-04648576

HAL Id: hal-04648576

<https://hal.science/hal-04648576v1>

Submitted on 30 Jul 2024

HAL is a multi-disciplinary open access archive for the deposit and dissemination of scientific research documents, whether they are published or not. The documents may come from teaching and research institutions in France or abroad, or from public or private research centers.

L'archive ouverte pluridisciplinaire **HAL**, est destinée au dépôt et à la diffusion de documents scientifiques de niveau recherche, publiés ou non, émanant des établissements d'enseignement et de recherche français ou étrangers, des laboratoires publics ou privés.

Adaptation to host in *Vibrio vulnificus*, a zoonotic pathogen that causes septicemia in fish and humans

Carla Hernández-Cabanyero 1

Chung-Te Lee 2

Verónica Tolosa-Enguis 1

Eva Sanjuán 1

David Pajuelo 1+

Felipe Reyes-López 3

Lluís Tort 3

Carmen Amaro 1

1 ERI-Biotecmed, University of Valencia, Dr. Moliner, 50, 46100, Valencia, Spain.

2 Department of Microbiology and Immunology, College of Medicine, National Cheng Kung University, Tainan, Taiwan.

3 Department of Cell Biology, Physiology and Immunology, Universitat Autònoma de Barcelona, 08193, Bellaterra, Spain

Summary

Vibrio vulnificus is a siderophilic pathogen spreading due to global warming. The zoonotic strains constitute a clonal-complex related to fish farms that are distributed worldwide. In this study, we applied a transcriptomic and single gene approach and discover that the zoonotic strains bypassed the iron requirement of the species thanks to the acquisition of two iron-regulated outer membrane proteins (IROMPs) involved in resistance to fish innate immunity. Both proteins have been acquired by horizontal gene transfer and are contributing to the successful spreading of this clonal-complex. We have also discovered that the zoonotic strains express a virulent phenotype in the blood of its main susceptible hosts (iron-overloaded humans and healthy eels) by combining a host-specific protective envelope with the common expression of two toxins (VvhA and RtxA1), one of which (RtxA1) is directly involved in sepsis. Finally, we found that both IROMPs are also present in other fish pathogenic species and have recently been transmitted to the phylogenetic lineage involved in human primary sepsis after raw seafood ingestion. Together our results highlight the potential hazard that the aquaculture industry poses to public health, which is of particular relevance in the context of a warming world.

Introduction

Vibrio vulnificus is a zoonotic pathogen that inhabits temperate, tropical and subtropical aquatic ecosystems whose geographical and epidemiological distribution is spreading alarmingly to traditionally cold areas due to global warming (Oliver, 2015; Baker-Austin and Oliver, 2018). This bacterium infects humans or fish (especially farmed fish species) either by contact or by ingestion causing a variety of diseases called

vibriosis (Amaro et al., 2015; Oliver, 2015). If the infected host is a human risk patient or a farmed eel, the pathogen can invade the bloodstream, resist the innate immunity and cause death by sepsis (Horseman and Surani, 2011; Oliver, 2015). Epidemiological studies suggest that the main risk factor predisposing to sepsis caused by *V. vulnificus* in humans is a high iron concentration in blood due to various pathologies (Horseman and Surani, 2011; Oliver, 2015) while septicemia in eels occurs in healthy specimens (Amaro et al., 2015).

A recent phylogenomic study classified *V. vulnificus* into five phylogenetic lineages plus one pathovar (pv. *piscis*), which includes all the strains harbouring a fish virulence plasmid (pVvBt2) (Roig et al., 2018). This pathovar is further subdivided into three serovar-related subgroups, one of which, serovar E, constitutes a zoonotic clonal-complex (Sanjuán et al., 2011; Roig et al., 2018). Currently, the zoonotic clonal-complex is present worldwide and includes strains isolated over a 40-year period from humans, diseased/healthy animals and water-samples (Roig et al., 2018). The most relevant virulence factors described in the zoonotic clonal-complex are the RtxA1 toxin, involved in invasion and death by sepsis (Jeong and Satchell, 2012; Lee et al., 2013; Callol et al., 2015; Murciano et al., 2017), a capsule, involved in resistance to human serum, and the O-antigen, conferring resistance to eel serum (Amaro et al., 1994; Amaro et al., 1997). No role has been assigned to VvhA, an hemolysin that seems to have an additive function to RtxA1 in strains from which it has been analysed, all of which belong to lineage 1 (Jeong and Satchell, 2012). Recently, Pajuelo et al. (2016) described the iron stimulon and the Fur (ferric uptake regulator) regulon in the zoonotic clonal-complex and demonstrated that the proportion of capsular antigen vs O-antigen changes in response to iron content in the external medium.

The aim of this work was to gain insights into the mechanisms that *V. vulnificus* uses to cause sepsis in hosts as evolutionarily distant as humans and fish and to evaluate its implication in the epidemiology of this bacterial species in a warming world. To this end, we analysed the transcriptome of a zoonotic strain (Pajuelo et al., 2016) in serum from each host [ex vivo model of septicemia (Sanjuán and Amaro, 2004)] and validated the results by genetic (RT-qPCR) and phenotypic assays (metabolic, virulence, resistance to innate immunity, etc.) with selected mutants. Our results show the association between high iron content in blood and septicemia caused by the zoonotic clonal-complex in humans, but not in eels, thus highlighting the role of iron as one of the external markers triggering a host-adapted virulent phenotype. This phenotype consists basically of a generalist but host-dependent protective envelope plus the common overexpression of RtxA1 and VvhA. In the case of humans, the envelope would be enriched in the capsule, while in eels it would contain two outer membrane proteins (OMPs) conferring the specific ability to resist fish innate immunity. Interestingly, the genes encoding both

proteins have been recently transmitted to other phylogenetic groups within *V. vulnificus*. This horizontal transmission most likely contributes to the persistence of this pathogenic species in and between hosts in nature, therefore increasing the probability of human infections, especially in a warming world.

Results

Transcriptome in serum and phenotypic validation

We analysed the differentially expressed genes of strain R99 (Supporting Information Table S1) in eel serum, human serum, and human serum supplemented with iron (ironoverloaded human serum) [to mimic the bloodstream of a risk patient affected from haemochromatosis (Murciano et al., 2017)] (Fig. 1). Remarkably, the affected cellular processes were the same than those revealed by the transcriptomic study performed by Pajuelo et al. (2016). Supporting Information Figure S1 shows the number of differentially expressed genes in serum in common with iron stimulon and/or Fur regulon (Pajuelo et al., 2016), Supporting Information Tables S2–S4 show the differentially expressed genes in each serum, Tables 1–3 provide a selection of differentially expressed genes grouped by putative function, and Table 4 provides a comparison between fold-change values obtained by hybridization with the R99-specific microarray and by RT-qPCR.

Eel serum. We obtained strong evidence of a switch from aerobic to anaerobic metabolism in eel serum vs minimal medium (M9 supplemented with casamino acids) (Miller, 1972), mainly highlighted by the upregulation of *arcA* (anaerobic metabolism repressor) together with most of the genes for nitrate/nitrite respiration (Table 1 and Supporting Information Table S2). This result was phenotypically confirmed by a dissimilatory reduction of nitrate/nitrite in eel serum but not in CM9 at 6 h post-inoculation (Supporting Information Fig. S2A). The pathogen upregulated *lrp*, encoding a master regulator for N-compound metabolism, plus multiple genes for organic nitrogen organic compound uptake/transport/metabolism (Table 1 and Supporting Information Table S2) (Brinkman et al., 2003; Ho et al., 2017). In parallel, genes for regulators/sensors related to nitrogen, phosphorus

and nucleoside starvation (*cytR*) were also differentially expressed in eel serum vs CM9 (Table 1 and Supporting Information Table S2). Regarding CytR, it has also been described to regulate competence (Antonova et al., 2012), which is activated in *V. cholerae* by chitin or their derivative amino sugars (e.g. N-acetyl-glucosamine) (Meibom et al., 2005). Accordingly, the main competence regulator TfoX (Metzger and Blokesch, 2016), and genes for specific N-acetyl-glucosamine uptake/transport were also upregulated concomitantly with the downregulation of two genes for amino sugar metabolism repressors (*uxuR* and *kdgR*) (Niecekarz et al., 2017) (Table 1 and Supporting Information Table S2). R99 strain also downregulated *fur* and upregulated most of the genes for vulnibactin biosynthesis/uptake/transport, as well as for transport/utilization of the host's heme compounds and fish transferrin (Table 1 and Supporting Information Table S2).

We obtained strong evidences of cell damage and stress response in eel serum, because multiple genes related to membrane regeneration were highly upregulated as well as genes for different stress-related protective proteins (Mathur and Waldor, 2004; Mathur et al., 2007; Phadtare and Severinov, 2010; Manganelli and Gennaro, 2017) (Table 1 and Supporting Information Table S2). Remarkably, the R99 strain seemed to respond specifically against oxidative/ nitrosative stress by downregulating genes for two repressors, *ohr* and *nsr*, and upregulating an activator, *norR*, together with genes for various hydroperoxidases, a glutathione synthetase and a hydroxylamine reductase (Fuangthong et al., 2001; Rodionov et al., 2005) (Table 1 and Supporting Information Table S2). In addition, a significant proportion of the genes involved in flagellum biosynthesis were downregulated in eel serum (Table 1 and Supporting Information Table S2). This result was also phenotypically confirmed as strain R99 was non-motile on eel serum supplemented with 0.3% agar, while it was motile on CM9-agar (Supporting Information Fig. S2B). Finally, some genes for capsule/O-antigen biosynthesis, *vvhA*, *rtxA1* plus genes for regulators involved in toxin production, quorum sensing (QS) and a gene for a DNA-binding H-NS protein (silencing protein mainly for mobile genetic elements transcription) were also differentially expressed (Table 1 and Supporting Information Table S2).

Interestingly, more than 90% of the mentioned genes belong to iron stimulon and/or Fur regulon (Table 1 and Supporting Information Table S2).

Human serum. Strain R99 was unable to multiply efficiently in human serum, inability that was reversed by adding iron (Supporting Information Fig. S2C). Consequently, few differentially expressed genes were upregulated in human serum vs CM9, specifically only those related to siderophore biosynthesis/uptake, resistance/protection against oxidative stress, and MSHA biosynthesis, most of which also overexpressed in eel serum (Table 2 and Supporting Information Table S3). In contrast, a more diverse transcriptomic response was observed in iron-overloaded human serum vs CM9 (Table 3 and Supporting Information Table S4), where most of the differentially expressed genes were oppositely regulated to what we observed in eel serum, i.e. genes for nitrite/nitrate respiration, siderophore biosynthesis/uptake, flagellum biosynthesis and motility (Tables 1 and 3 and Supporting Information Tables S2 and S4). We phenotypically confirmed most of these transcriptomic evidence as strain R99 was unable to respire nitrate/nitrite and was more motile in iron-overloaded human serum supplemented with 0.3% agar than in CM9-agar (or eel serum supplemented with 0.3% agar) (Supporting Information Fig. S2B). As in eel serum, R99 seemed to present an anaerobic respiratory metabolism in ironoverloaded human serum, probably based on organic compounds (i.e. fumarate) and using glycogen/glucan and derived sugars (e.g. maltose) as the main energy and carbon sources (Table 3 and Supporting Information Table S4). This result was partially confirmed by a significant positive result for increased growth after exogenous maltose addition in iron-overloaded human serum but not in CM9 (or human serum) (Supporting Information Fig. S2D).

The pathogen also upregulated genes for protection against different stresses, regeneration of damaged proteins, lipids and membranes in iron-overloaded human serum, many of which differed from those found in eel serum (Tables 1 and 3 and Supporting Information Tables S2 and S4). As in eel serum, *vvhA* and *rtxA1* were also differentially expressed in iron-overloaded human serum, as were some genes for LPS/capsule biosynthesis (Table 3 and Supporting Information Table S4). Finally, genes for different transcriptional regulators, most not found in eel serum, were also differentially expressed in iron-overloaded human serum [i.e. HlyU, the main activator of *rtxA1* (Liu et al., 2011); VieB, a repressor for the virulence activator VieA (Lee et al., 1998; Mitchell et al., 2015); SmcR, the main QS regulator (Kim et al., 2013); QseB, a regulator that responds to iron and QS signals (Weigel et al., 2015); and VpsT, a biofilm formation activator (Krasteva et al., 2010)] (Table 3 and Supporting Information Table S4).

Approximately, a 90% of all the above genes belong to iron stimulon and/or Fur regulon (Table 3 and Supporting Information Table S4).

Virulence factors differentially expressed in serum

Toxins. *vvhA* and *vvhB* [encoding a secretory protein for VvhA (Yamamoto et al., 1990)], were the most strongly upregulated genes in eel serum, while *rtxA1* and *rtxC* [encoding an enzyme for RtxA1 post-transcriptional modification (Satchell, 2011)] were downregulated (Table 1 and Supporting Information Table S2). We demonstrated that *vvhA* is involved in virulence and *in vivo* survival in the blood since both LD₅₀ (Table 5) and bacterial counts in the blood from bath-infected eels (Fig. 2A) were significantly impaired in a mutant strain deficient in *vvhA*. To uncover the role of VvhA in survival in the blood, we evaluated the hemolysis by R99 vs $\Delta vvhA$ strains in artificial eel blood (eel serum supplemented with erythrocytes, see Experimental procedures) as well as the transcription of *vvhA* by R99 strain for 6 h postinfection. In these experiments, we also included the mutants $\Delta rtxA1$ and $\Delta vvhA\Delta rtxA1$ as controls, as RtxA1 can also cause haemolysis *in vitro* (Wright and Morris, 1991; Kim et al., 2008). First, we found that *rtxA1* was upregulated when erythrocytes were added to eel serum (fold-change value changing from -2.6 in eel serum to 5.8 in artificial eel blood at 6 h post-infection), which correlated with previous results obtained *in vivo* (Lee et al., 2013). Second, *vvhA* was transcribed before *rtxA1* and appeared to be mainly responsible for hemolysis at 6 h post-infection (Fig. 2B). This result correlated well with those obtained *in vivo*, as *vvhA* and *rtxA1* were upregulated in the blood of bath-infected eels (*vvhA* at 3 h and *rtxA1* at 9 h post-infection with fold induction values of 8.7 ± 0.5 and 3 ± 0.2 respectively). We repeated the experiments with artificial iron-overloaded human blood [ironoverloaded supplemented with erythrocytes (see Experimental procedures)] and observed that *rtxA1* and *vvhA* were transcribed in parallel from the beginning of the experiment, achieving a similar fold induction value at 6 h post-infection, however in this case, the hemolysis at 6 h seemed to be mainly due to RtxA1 (Fig. 2B).

Envelope polysaccharides. Capsule and O-antigen are involved in resistance to the human and fish innate immunity (Amaro et al., 1994; Amaro et al., 1997).

Transcriptomic results showed that multiple genes related to both LPS and capsule biosynthesis were differentially expressed in serum (Tables 1 and 3 and Supporting Information Tables S2 and S4; Fig. 3A). Therefore, we analysed the polysaccharide profile from R99 strain grown in eel serum, human serum and iron-overloaded human serum. The

pathogen changed the proportion of capsule vs O-antigen in human serum, producing more capsule in iron-overloaded human serum (Fig. 3B). In case of eel serum, the pathogen seemed to produce an intermediate pattern with similar amounts of capsule and O-antigen, without major differences to those seen in CM9 (Fig. 3B).

Remarkably, the O-antigen contained the high/medium molecular weight bands previously described to be involved in resistance to eel complement (Amaro et al., 1997). Although we could not estimate free iron in serum, we determined the total iron (free and protein associated) and found that eel serum contains more iron (1.1 mg l^{-1}) than human serum (0.75 mg ml^{-1}), suggesting that eel serum is less restrictive.

Vep07. One of the upregulated genes in both eel serum and human serum was *vep07* (Supporting Information Tables S2 and S3), a gene encoding a hypothetical protein involved in virulence in eels but not in mice (Lee et al., 2008). An *in silico* analysis of this protein [using two bacterial lipoprotein prediction programs, LipoP (Juncker and Willenbrock, 2003) and DOLOP (Madan and Sankaran, 2002)] revealed that Vep07 is probably an outer membrane (OM) lipoprotein. Therefore, we analysed the presence of Vep07 in different bacterial fractions by immunostaining with the antibody antiVep07 and confirmed that Vep07 is an OM protein (OMP) of approximately 55 kDa that is regulated by iron as it was only expressed under iron-restricted conditions, either imposed by an iron chelator or by eel serum (Fig. 4A). Additional *in vitro* and *ex vivo* experiments showed that *vep07* was mainly transcribed during the first hours of growth both in eel serum and iron deficient minimal medium (CM9 supplemented with human transferrin) (Fig. 4B). To determine the role of Vep07 in virulence, we used R99 and Δ *vep07*, *cv**vep07*, Δ *ftbp* and Δ *ftbp* Δ *vep07* strains in a series of *in vivo* and *ex vivo* assays (Supporting Information Table S1). Similar to Δ *ftbp* (Pajuelo et al., 2015), Δ *vep07* was severely impaired in virulence for eels, growth in eel blood and resistance to eel serum and did not show changes in virulence for mice and resistance to human serum (Table 5). The inhibitory effect of eel serum on Δ *vep07* was reversed by the inactivation of both the alternative and classical pathways of complement or by the inactivation of the alternative pathway alone, but it was not reversed when iron was added or when the classical pathway alone was inactivated (Table 6). As expected, the inhibitory effect of eel serum on Δ *ftbp* was only reversed by adding iron (Table 6). Additionally, Δ *vep07* was sensitive to phagocytosis (Table 5). The sensitivity to complement and phagocytosis was reversed by the inclusion of the gene *in trans* in the mutant (Table 5). The double mutant in *ftbp* and *vep07* was completely avirulent for eels, died in eel serum and was still sensitive after either iron addition or eel complement inactivation (Tables 5 and 6). Finally, *in vivo* experiments of colonization/invasion showed that Δ *vep07* was

impaired in internal colonization not only for blood but also for the other internal organs we analysed (Fig. 4C).

ftbp has been reported to be horizontally transmitted to other fish pathogenic bacteria (Pajuelo et al., 2015). Therefore, we analysed the presence of *vep07* in other genomes and constructed a phylogenetic tree for all the found sequences (Fig. 4D). *vep07* was present together with *ftbp* not only in *pv. piscis* but also in recent isolates of *V. vulnificus* from other phylogenetic lineages not previously linked to disease in fish (Roig et al., 2018), as well as in the plasmid of one *V. harveyi* strain isolated from diseased seabass. Interestingly, two main groups were established on the basis of *vep07* variability, one group with all the *pv. piscis* isolates which have the ability to infect eels, and the other one with *V. vulnificus* isolates from the other phylogenetic groups together with the *V. harveyi* strain (Fig. 4D).

Discussion

In this work, we aimed to characterize the strategies used by *V. vulnificus* to survive within hosts as evolutionarily distant as human and fish, in order to gain a better understanding of the epidemiology of this bacterial species in a warming world. Our main conclusions from the transcriptomic study performed in serum plus the complementary assays are summarized in the models presented in Figs 5 and 6. Because approximately one out of every two differentially expressed genes in the serum belong to the previously described Fur regulon and/or iron stimulon (Pajuelo et al., 2016), we selected the most relevant differentially expressed genes encoding regulators, sensors, and virulence factors, all of which (with a very few exceptions) belong to one or both regulatory systems. Figure 5 shows the predicted regulatory networks, external stimuli and phenotype presented by zoonotic strains growing in serum, while Fig. 6 summarizes the main virulence factors that the pathogen would express in the blood per susceptible host, healthy eels and high-risk patients (those with high iron levels in blood), as well as its putative role in virulence.

Zoonotic clonal-complex activates an anaerobic metabolism to survive and grow in the blood regardless of the host and iron levels (Fig. 5) and even oxygen levels, since the values of dissolved oxygen were similar in all the inoculated sera and control media after 6 h of incubation ($1-2 \text{ mg l}^{-1} \text{ O}_2$). This anaerobic metabolism would probably be based on N-compound utilization and nitrate/nitrite respiration in eels or glycogen (maltose)-related compound utilization and organic compounds respiration (such as fumarate) in high-risk human patients. Although the external signals triggering this metabolic switch are unclear, it seems reasonable to hypothesize that membrane attack by complement and microcidal peptides (common to fish and human sera) would disrupt proton motive force, thus activating *pspABC* system [belonging to Fur regulon

and upregulated in both sera, especially in iron-overloaded human serum (Tables 1–3)]. This in turn would activate anaerobic metabolism as it has been described for *Escherichia coli* (Jovanovic et al., 2006) (Fig. 5). In addition, the upregulation of *arcA* in eel serum [linked to the upregulation of *pspABC* (Manganelli and Gennaro, 2017)], as well as the upregulation of *qseB* in iron-overloaded human serum, could also contribute to anaerobic metabolism activation. Indeed, QseB has been described as an activator of anaerobic metabolism in iron-overloaded media in response to catecholamines (Weigel et al., 2015) as well as an activator of motility (Weigel and Demuth, 2016), a phenotype that is induced in iron-overloaded human serum (Table 3 and Supporting Information Fig. S2B). Our transcriptomic results also suggest that Fur would play a central role in determining the preferable nutrient to be used, either as apo-Fur through Lrp (Ho et al., 2017) in eel serum or as holo-Fur through unknown pathways in iron-overloaded human serum as all the glycogen metabolism-related differentially expressed genes belong to the Fur regulon (Supporting Information Table S4 and Fig. 5). The ability to respire nitrate/nitrite in eel blood provides the pathogen with an additional advantage as the protective mechanisms against nitric oxide (a respiration byproduct) that are concomitantly activated (Table 1) would protect it against this important microcidal molecule produced by the host, contributing to the high virulence of the zoonotic clonal-complex for eels.

Besides this metabolic adaptation, our transcriptomic results also suggest that the zoonotic clonal-complex responds to more signals of nutrient starvation in eel serum than in iron-overloaded human serum (Tables 1 and 3). We highlight that the zoonotic clonal-complex would respond in eel serum to iron and nucleotide starvation, which would involve Fur and CytR [belonging to Fur regulon (Pajuelo et al., 2016)], respectively, resulting in the upregulation of different genes involved in the uptake of both kinds of nutrients (i.e. vibriobactin biosynthesis, receptors for different exogenous iron sources, and nucleoside transporters) (Supporting Information Tables S2 and S4). As a secondary consequence of *cytR* upregulation, competence could be activated, at least partially, in eel serum, which is supported by the upregulation of *tfoX* (Fig. 5). We hypothesize that this putative competence activation could indicate that the zoonotic clonal-complex might activate this state in its natural habitat, i.e. fish mucosae (Carda-Diéguez et al., 2017), as *V. cholerae* does (Metzger and Blokesch, 2016), and that iron starvation could play a role in the process as both eel serum and fish mucosae are iron restricted environments (Pajuelo et al., 2015; Carda-Diéguez et al., 2017).

The zoonotic clonal-complex expresses a toxin phenotype in the blood of its susceptible hosts, which is based on VvhA plus

RtxA1 production. Our transcriptomic and phenotypic results suggest that iron, Fur, SmcR and HlyU could play a significant role in the activation of this toxic phenotype (Fig. 5). In case of high-risk patients, RtxA1 and VvhA could act additively in the blood as both genes were upregulated in iron-overloaded human serum and were transcribed in parallel and exponentially in artificial iron-overloaded human blood during the 6 h of incubation we analysed. A role for this additive function in blood invasion from the intestine has already been suggested for *V. vulnificus* strains, other than the zoonotic ones (Jeong and Satchell, 2012). In addition, the regulation of *smcR*, *fur* and *hlyU* in iron-overloaded human serum was as expected according to both the observed toxin gene transcription and the published literature (Shao et al., 2011; Kim et al., 2013) (Fig. 5). In consequence, a highly toxic phenotype would be induced in the zoonotic clonal-complex when infecting high-risk patients, which agrees with clinical data on human septicemia (Horseman and Surani, 2011; Oliver, 2015).

The scenario was different in the case of eels, as the results were unexpected. First, *rtxA1*, a gene essential for eel death by sepsis (Lee et al., 2013), was downregulated in eel serum, while *vvhA*, a gene with an unknown role in eel virulence, was one of the most strongly upregulated (Fig. 5). The complementary experiments performed in artificial eel blood and *in vivo* demonstrated that the *rtxA1* transcription requires contact of the bacteria with host cells as previously suggested for the function of this toxin (Kim et al., 2008), and supporting previous results (Lee et al., 2013). Second, *hlyU* was downregulated which correlated with *rtxA1* transcription but not with *vvhA* transcription, suggesting that iron starvation, in the absence of HlyU, could trigger *vvhA* transcription through an unknown regulatory pathway (Fig. 5). Additional experiments to unravel the role in eel virulence of *vvhA* by using a mutant and the corresponding complemented strain demonstrated that *vvhA* is a virulence gene probably involved in early fitness in eel blood. Interestingly, *vvhA* was transcribed before *rtxA1*, both in artificial eel blood and *in vivo*, and in both cases the fold-change/induction value was much lower than that observed in eel serum at 6 h post-infection (Fig. 2B). All these results highlight a new hypothesis on hemolysin transcription *in vivo*: the temporality in the transcription of *rtxA1* and *vvhA* could depend on changes in iron concentration in the bacteria's surrounding environment. A model summarizing the role of both toxins per host is shown in Fig. 6. This model incorporates the hypothesis that VvhA (transcribed first in eel serum) would lyse erythrocytes and create an iron-rich microenvironment (heme) that would favour the transcription of *rtxA1* in eel blood. More studies are necessary to prove these hypotheses.

The zoonotic clonal-complex produces a protective envelope in the blood against complement from each susceptible host in terms of capsule vs O-antigen ratio. Our transcriptomic and phenotypic results suggest that iron and Fur would have a role in the production of this protective envelope as all the identified capsule/LPS biosynthetic differentially expressed genes belonged to the Fur regulon and most of them also to iron stimulon (Supporting Information Tables S2 and S4 and Fig. 5). Accordingly, the selected zoonotic strain produced a capsule enriched envelope in iron-overloaded human serum and an envelope without capsule but O-antigen enriched in human serum (Fig. 3B), which supports the hypothesis of Pajuelo et al. (2016) regarding the role of iron in capsule/O-antigen production. The fact that the zoonotic clonal-complex is unable to produce capsule in human serum would by itself explain why this pathogen does not cause septicemia in healthy patients as the invading bacteria would be destroyed by human complement (Amaro et al., 1994). In partial accordance, the envelope produced in eel serum by the analysed strain contained both capsule and high/medium molecular weight O-antigen, both participating in protection against eel complement (Biosca et al., 1993; Amaro et al., 1997). The role of capsule and O-antigen (LPS) in human and fish septicemia is summarized in Fig. 6.

Capsule production is inversely linked to the biofilm formation in *V. vulnificus* (Joseph and Wright, 2004; CasperLindley and Yildiz, 2014). Accordingly, we found that the biofilm formation was significantly higher ($p < 0.001$) in CM9 than in iron-overloaded human serum (values of Ab_{S540} after crystal violet staining of 0.29 ± 0.04 and 0.01 ± 0.001 respectively) confirming that the biofilm formation is downregulated in iron-overloaded human serum (Fig. 5). We also found transcriptomic evidences: i.e. the downregulation of *smcR*, linked to the downregulation of *vpsT*, an activator of the biofilm formation (Krasteva et al., 2010) plus the upregulation of *fur* linked to the downregulation of *vieB*, a repressor of *VieA*, which forms with *VieS* a two-component system that represses the biofilm formation (Mitchell et al., 2015).

The external envelope of the zoonotic clonal-complex contains two host-range related IROMPs that confer resistance to the innate immunity of specific fish species. These two proteins are Ftbp, a recently described receptor for eel transferrin that can bind transferrin from seabass as well (Pajuelo et al., 2015; unpublished result), and *vep07*, encoding a multifunctional OMP (probably a lipoprotein) conferring resistance to eel complement, activated by the alternative pathway, and phagocytosis. We propose the description, name 'Fish Phagocytosis and Complement Resistance Protein' [Fpcrp] for this protein. Both proteins would constitute a 'survival in fish blood kit' conferring both specific adaptation to resist the fish innate immunity and high virulence for healthy eels (Fig. 6). Our hypothesis is that Fpcrp binds an unknown fish

complement inhibitor, thus preventing bacterial killing and efficient opsonization/ phagocytosis. Incubation of purified rVep07 with albumin-free eel serum and further identification of the ligand by liquid chromatography and tandem mass spectrometry (LC-MS/MS) (Pajuelo et al., 2015) were unsuccessful, probably because the eel protein target has not yet been sequenced (results not shown). Future analysis of the eel serum proteome is ongoing in order to identify the Fpcrp ligand. The role of both proteins in eel sepsis is summarized in Fig. 6.

The gene *fpcrp*, as *ftbp*, has been acquired by HGT probably in the fish farm environment. As expected, a homologous gene to *fpcrp* was present together with *ftbp* in all the *pv. piscis* strains sequenced to date with an identity and coverage of almost 100% and it was also in a conjugative-virulence plasmid (pVh1) (Pajuelo et al., 2015) harboured by one strain of *V. harveyi* isolated from a diseased farmed seabass (Pajuelo et al., 2015). Surprisingly, both genes were also present in other recently isolated *V. vulnificus* strains, one from a woman infected after ingestion of raw fish (sushi) and the other from a fish farm water (Danin-Poleg et al., 2015; Chung et al., 2016) (Fig. 4D). Both strains belong to lineage 1 (Roig et al., 2018), the most dangerous phylogenetic group from the public health perspective because it includes most of the isolates related to primary septicemia in humans (Roig et al., 2018). Further, the phylogenetic analysis of *fpcrp* divided the strains in two groups, one that included the *pv. piscis* strains and the other that included the new strains belonging to lineage 1 together with the *V. harveyi* isolate. Therefore, the differences in the gene sequences between both groups of strains could indicate that the new *V. vulnificus* isolates would have acquired the gene from a bacterium other than the zoonotic group and closer to *V. harveyi* probably in fish farms environments.

Conclusions

In summary, we have unravelled some of the mechanisms that enable the zoonotic strains of *V. vulnificus* to cause septicemia in hosts as evolutionary distant as humans and fish and clarified the link between virulence and iron content in the blood. First, zoonotic strains would only be able to cause septicemia in humans with elevated iron levels in blood because, only under iron excess would be able to produce a capsule enriched envelope that would allow it to multiply efficiently in the blood and to express the highly toxic phenotype responsible for patient death by sepsis. Second, *V. vulnificus* has horizontally acquired a 'survival in fish blood kit' that allows it to resist fish innate immunity and multiply in the blood expressing a toxic phenotype responsible for animal death by sepsis. If the disease occurs in a fish farm, it could lead to an outbreak and the subsequent amplification of the genetically transformed clone. In fact, we have found evidences that this kit has already

been transmitted to the most dangerous phylogenetic group, the one related to primary sepsis after raw seafood ingestion. In conclusion, our results highlight the risk that the aquaculture industry poses to public health, especially in the case of such zoonotic pathogens as *V. vulnificus* whose multiplication and spreading to new areas is being favoured by global warming.

Experimental procedures

Strains, media and bacterial growth

Bacterial strains (Supporting Information Table S1) were grown in TSA-1 (TSA, 1% NaCl), CM9 (Miller, 1972), CM9+ Tf [CM9 + 10 μ M human transferrin (Sigma-Aldrich)], CM9-Fe [CM9 + 200 or 400 μ M of the iron chelator 2,2' bipyridyl (Sigma-Aldrich)], CM9+Fe (CM9 + 100 μ M FeCl₃), eel serum [obtained as previously described (Lee et al., 2013)], iron-overloaded eel serum (eel serum + 2.5, 5 or 100 μ M FeCl₃), human serum (Sigma-Aldrich), and ironoverloaded human serum [human serum +100 μ M FeCl₃ (Murciano et al., 2017)]. Unless clearly specified, 2.5 ml of each serum/broth were inoculated with washed bacteria (10^5 CFU ml⁻¹) and incubated with agitation (50 rpm) at 28°C (eels) or 37°C (humans). Bacterial growth was monitored as CFU ml⁻¹ at regular time intervals.

Animal maintenance and extraction of blood, serum, erythrocytes and phagocytes.

Mice (6- to 8-week-old female BALB/c mice, Charles River, France) and farmed eels (European eel, *Anguilla anguilla*, purchased from a local eel farm that does not vaccinate against *V. vulnificus*) were maintained and handled in the facilities of the Central Service for Experimental Research (SCSIE) of the University of Valencia (Spain) according to that specified in ethic statement. Blood and serum as well as erythrocytes and phagocytes were obtained from eels as previously described (Lee et al., 2013). Human blood was obtained from volunteers as described in ethic statement.

Virulence, colonization and invasion assays

Virulence for mice and eels was determined as LD₅₀ (Reed and Muench, 1938) after infecting the animals (around 20 g) with serial bacterial 10-fold dilutions in PBS either by intra-peritoneal injection (groups of six animals per dose) or immersion (only eels: groups of 10 animals per dose) as previously described (Amaro et al., 1994; Amaro et al., 1995). Mortalities were only considered if the inoculated strain was recovered as a pure culture from internal organs. *Eel colonization and invasion assays* were performed by immersion of groups of 24 eels (around 50 g) per strain in an infective bath adjusted at the LD₅₀ for R99 strain (Amaro et al., 1995). Three live eels per group were randomly sampled at 0, 9, 24 and 72 h, sacrificed and sampled for bacterial counts (CFU

ml⁻¹) and for quantification of selected genes by RT-qPCR according to Pajuelo et al. (2015) (see next section). In all cases, an extra group was infected with sterile PBS as a control (Amaro et al., 1995).

Transcriptomic experiments and data analysis

Bacterial transcriptome was analysed in serum vs CM9 after 6 h of incubation (Abs₆₂₅ 0.3) (serum complement starts to be significantly inactivated from 6 h of incubation) according to Pajuelo et al. (2016). Briefly, total RNA was extracted using the Direct-zol™ RNA Miniprep kit (Zymo), subjected to DNase treatment using the TURBO™ DNase (Ambion) and cleaned using the RNA Clean & Concentrator™ kit (Zymo). Only samples with a RIN \geq 7.5 (measured using a 2100 Bioanalyzer, Agilent) were selected to get labelled cDNA that was hybridized with the R99-specific microarray (Pajuelo et al., 2016). The data were analysed using the Genespring 14.5 GX software (Agilent technologies) with 75% percentile normalization for the following comparisons: eel serum vs CM9, human serum vs CM9 and iron-overloaded human serum vs CM9. Student's *t*-test ($p < 0.05$) available in Genespring software was applied to reveal transcriptomic profile differences between the conditions. Results are presented as averages of the fold change [the ratio between two conditions (serum vs CM9) which gave the absolute ratio of normalized intensities between the average intensities of three independent samples]. The same samples used for the microarray analysis as well as the samples from eel tissues were analysed by RT-qPCR to calculate the expression of the selected genes (primers listed in the Supporting Information Table S5). The recA gene was used as standard and the fold induction ($2^{-\Delta\Delta Ct}$) for each gene was calculated according to Livak and Schmittgen (2001).

Resistance to innate immunity in serum and blood

Bacteria were incubated (10^3 CFU ml⁻¹) in 96-well plates (NUNC) containing 200 μ l of each sample (serum/blood) for 4 h. The effect of iron or complement inactivation on the bacterial survival was determined by comparing the bacterial growth in fresh vs treated serum. Serum + iron and inactivated serum were obtained as previously published (Sunyer and Tort, 1995; Pajuelo et al., 2015; Murciano et al., 2017). The survival index after 4 h of incubation (SI_{4h}) was determined (Lee et al., 2013).

Resistance to phagocytosis

Blood eel phagocytes were seeded in poly-L-lysine treated 96-well plates (10^5 cells/well). Bacteria were added in a multiplicity of infection (moi) of 10 in a final volume of 200 μ l/well. Bacterial counts were performed at 0 and 90 min to

calculate the percentage of bacteria that survived after phagocytosis (Lee et al., 2013).

Haemolysis

Artificial blood was prepared by adding erythrocytes (10^6 cells ml^{-1}) to serum (either eel or iron-overloaded human serum respectively). Artificial blood was seeded in 96-well plates and bacteria were added at a moi of 0.5 in a final volume of 200 μl well $^{-1}$. Erythrocytes counts were performed at 0, 1.30, 3 and 6 h post-infection to calculate the percentage of cell lysis. In parallel, samples for RNA extraction and quantification of *vwA* and *rtxA1* were taken.

Motility

Motility was assayed on CM9, eel serum, human serum and iron-overloaded human serum, 0.3% agar (wt/vol) as previously described by Pajuelo et al. (2016).

Metabolism

The ability to respire nitrate/nitrite was determined in strain R99 grown for 6 h in 96-well plates containing 200 μl of CM9, eel serum or iron-overloaded human serum by adding NIT1 and NIT2 reagents (API[®], BioMérieux) to each well. *The ability to grow from exogenous maltose* added to CM9, human serum and ironoverloaded human serum was determined by growing R99 in glass tubes and after 6 h of growth 0.2% (wt/vol) maltose was added. Growth was measured as bacterial counts (CFU ml^{-1}) at 0 and 30 min after the addition of maltose.

Envelope analysis

Surface cell-associated-polysaccharides (LPS plus capsule) of R99 were obtained as described by Hitchcock and Brown (1983). About 10 μg of cell-associated-polysaccharides, quantified using the Total Carbohydrate Assay Kit (BioVision), were separated by SDS-PAGE, transferred onto a PVDF membrane and subjected to immunoblot analysis with antibodies against R99 cell envelopes (Amaro et al., 1994). The blots were developed following incubation with appropriated dilution of horseradish peroxidase-conjugated secondary antibodies using Immunobilon Western Chemiluminescent HRP Substrate (Millipore).

Biofilm production

R99 was grown in glass tubes containing 2 ml of CM9 or iron-overloaded human serum and biofilm production was quantified by staining with crystal violet (Pajuelo et al., 2016) at 24 h post-incubation.

Isolation of $\Delta\text{vep07}\Delta\text{ftbp}$ double mutant

The $\Delta\text{vep07}\Delta\text{ftbp}$ mutant was isolated by introducing the Δftbp DNA fragment which contains a 1407-bp in-frame deletion in *ftbp* into the Δvep07 mutant strain by the allelic exchange technique (Lee et al., 2008). Briefly, two DNA fragments amplified from R99 (Supporting Information Table S5) were cloned into a suicide plasmid, pCVD442 (Philippe et al., 2004) between *SacI* and *XbaI* sites, resulting a 1407-bp in-frame deletion in *ftbp*. The pCVD442 derivative with the deletion in *ftbp* was transformed into *E. coli* S17- λpir (Hanahan, 1983) and then transferred to the Δvep07 mutant strain by conjugation. The transconjugants were selected by ampicillin. The plasmid-integrated strain was then grown in LB containing 10% sucrose for 24 h and those resistant to 10% sucrose and sensitive to ampicillin were selected and confirmed by PCR and southern blotting as the double mutants (Pajuelo et al., 2015).

Generation of anti-rVEP07 serum and immunoblots

A 17 kDa partial recombinant Vep07 (rVep07) with a C-terminal six-histidine tag was overexpressed by inducing *E. coli* BL21 strains containing partial *vep07* gene cloned into pE30a with 1 mM IPTG for 16 h at 30C. Bacterial pellets disrupted by sonication and rVep07 were purified by affinity binding with the Ni^{2+} chelating sepharose (Chelating Sepharose[™] Fast Flow, GE Healthcare Life Sciences). Six weeks old female mice were immunized by subcutaneous injection with the 6xhistagged partial rVep07 accordingly to previously describe by Pajuelo et al. (2015). For the *vep07* gene translation studies, R99 was cultured in different iron conditions. A 5 μg of the insoluble fraction of each total cell lysate [quantified using the Pierce BCA Protein Assay Kit (Thermo Scientific)] were fractionated by SDSpolyacrylamide gel electrophoresis and then transferred onto a PVDF membrane. The membranes were probed with mouse anti-Vep07 serum. The blots were developed as described above.

Phylogenetic reconstruction

Phylogenetic trees were constructed with MEGA7 using the Maximum Likelihood method (Tamura, 1992; Kumar et al., 2016). Support for the groupings derived in these constructions was evaluated through bootstrapping using 1000 replicates (Felsenstein, 1985). Maximum-Likelihood trees were obtained using PhyML (Guindon and Gascuel, 2003). The best evolutionary model for the sequences according to jModelTest (Posada, 2008) and considering the Akaike information criterion (AIC) was the general time-reversible model of substitution with a gamma distribution (GTR + G) (Masatoshi and Kumar, 2000). The sequences were obtained from GenBank.

Statistical analysis

Data are presented as averages \pm standard error of at least three independent experiments. Statistical analysis was performed using SPSS 19.0. The significance of the differences between averages was tested by using the unpaired Student's t-test with a $p < 0.05$. When the effect of more than two independent variables was taken into account an ANOVA analysis was performed.

Ethic statement

Whole human blood was obtained from healthy volunteers at the University of Valencia. Assays were approved by the Institutional Committee on Human Research (project licence H1487946643442) following the Declaration of Helsinki. All assays involving animals were approved by the Institutional Animal Care and Use Committee and the local authority (Generalitat Valenciana), following European Directive 2010/63/EU and the Spanish law 'Real Decreto' 53/2013 and were performed in the SCSIE facilities by using the protocols 2016-USC-PEA-00033 type 2 (virulence in eels), 2014 VSC PEA 00195 type 2 (virulence in mice) and 2016-USC-PEA-00033 type 2 (colonization and invasion in eels). We also have a permission from Generalitat Valenciana to use eel for scientific research purposes.

Acknowledgements

The authors thank James D. Oliver for constructive criticism of the manuscript. This work has been financed by grants AGL2017-87723-P (co-funded with FEDER funds) from Ministry of Science, Innovation and Universities (Spain) and AICO/2018/123 from Generalitat Valenciana (Spain). Hernández-Cabanyero C has been financed by an FPI grant BES-2015-073117. The funders had no role in study design, data collection and analysis, decision to publish, or preparation of the article.

Supporting Information

Additional Supporting Information may be found in the online version of this article at the publisher's web-site:

Table S1. Bacterial strains and plasmids used to genetically modify the strains.

Table S2. Genes differentially expressed by *V. vulnificus* R99 strain in eel serum (ES) vs CM9 compared with those previously described in iron stimulon and Fur regulon (Pajuelo et al., 2016). *: present in iron stimulon or Fur regulon but with upside down regulation. **: only values of fold change $-2 \leq X \leq 2$ with a p-value cut-off of 0.05 were considered. +: gene up-regulated in eel serum; -: gene down-regulated in eel serum.

Table S3. Genes differentially expressed by *V. vulnificus* R99 strain in human serum (HS) vs CM9 compared with those previously described in iron stimulon and Fur regulon (Pajuelo et al., 2016). *: present in iron stimulon or Fur regulon but with upside down regulation. **: only values of fold change $-2 \leq X \leq 2$ with a p-value cut-off of 0.05 were considered. +: gene upregulated in human serum; -: gene down-regulated in human serum.

Table S4. Genes differentially expressed by *V. vulnificus* R99 strain in iron-overloaded human serum (HS+Fe) vs CM9 compared with those previously described in iron stimulon and Fur regulon (Pajuelo et al., 2016). *: present in iron stimulon or Fur regulon but with upside down regulation. **: only values of fold change $-2 \leq X \leq 2$ with a p-value cut-off of 0.05 were considered. +: gene up-regulated in ironoverloaded human serum; -: gene down-regulated in ironoverloaded human serum.

Table S5. Primers used in this study.

Figure S1. Number of differentially expressed genes in serum in common with iron stimulon and/or Fur regulon (previously described by Pajuelo et al. (2016)) represented as Venn diagrams.

Figure S2. Phenotypic assays to validate microarray data in serum. (A) Nitrate and nitrite respiration. Nitrate and nitrite respiration was measured with the API20E™ kit (Biomerieux, Spain) after incubation of R99 strain in eel serum (ES), ironoverloaded human serum (HS+Fe) and CM9. Positive results (red coloured wells) were obtained for eel serum at 3, 6 and 9 h post-incubation (a slight positive result could be observed in one of the replicates CM9 after 3 h of incubation). (B) Motility was measured as Motility rate (Mr) (colony surface in mm^2/\log of colony bacterial number in CFU ml^{-1}) according to Pajuelo et al. (2016). The assay was performed on plates of CM9- or serum-agar (0.3%). Eel serum (ES)-agar plates were incubated at 28C and iron-overloaded human serum (HS+Fe)-agar plates at 37C. Three independent biological replicates of each experiment were performed. CM9-agar column and bar present the average and standard error corresponding to 6 plates (3 incubated at 28C and 3 at 37C). *: significant differences ($P < 0.05$) serum-agar vs CM9-agar. (C) Survival in serum: R99 strain was inoculated in CM9 and serum (eel serum [ES], human serum [HS] or iron-overloaded human serum [HS+Fe [FeCl₃ 100 μM]]) and incubated for 6 h at 28C (CM9/ES) or 37C (CM9/HS/HS +Fe). % Survival: ratio bacterial counts at selected time intervals vs 0 h. Points and bars show the average and standard error from three independent experiments. *: significant differences ($P < 0.05$) serum vs CM9; #: significant differences ($P < 0.05$) HS vs HS+Fe. (D) Growth from exogenous maltose. R99 was grown in tubes containing CM9, human serum (HS) and iron-overloaded human serum (HS+Fe) for 6 h at 37C. Maltose (0.2% wt/vol) was added to half of the tubes and all the tubes were incubated for additional 30 min. %

Growth: ratio bacterial counts at 30 min vs 0 min postmaltose addition. Data are represented as a dot blot graph in which points are the averages and bars the standard deviations from three independent experiments. *: significant differences found with ANOVA analysis ($P < 0.05$) HS/HS+Fe vs CM9.

References

- Amaro, C., Biosca, E., Fouz, B., Alcaide, E., and Esteve, C. (1995) Evidence that water transmits *Vibrio vulnificus* biotype 2 infections to eels. *Appl Environ Microbiol* 61: 1133–1137.
- Amaro, C., Biosca, E., Fouz, B., Toranzo, A., and Garay, E. (1994) Role of iron, capsule, and toxins in the pathogenicity of *Vibrio vulnificus* biotype 2 for mice. *Infect Immun* 62: 759–763.
- Amaro, C., Fouz, B., Biosca, E.G., Marco-Noales, E., and Collado, R. (1997) The lipopolysaccharide O side chain of *Vibrio vulnificus* serogroup E is a virulence determinant for eels. *Infect Immun* 65: 2475–2479.
- Amaro, C., Sanjuán, E., Fouz, B., Pajuelo, D., Lee, C.T., Hor, L.I., and Barrera, R. (2015) The fish pathogen *Vibrio vulnificus* biotype 2: epidemiology, phylogeny, and virulence factors involved in warm-water vibriosis. *Microbiol Spectr* 3.
- Antonova, E.S., Bernardy, E.E., and Hammer, B.K. (2012) Natural competence in *Vibrio cholerae* is controlled by a nucleoside scavenging response that requires CytR-dependent anti-activation. *Mol Microbiol* 86: 1215–1231.
- Baker-Austin, C., and Oliver, J.D. (2018) *Vibrio vulnificus*: new insights into a deadly opportunistic pathogen. *Environ Microbiol* 20: 423–430.
- Biosca, E., Llorens, H., Garay, E., and Amaro, C. (1993) Presence of a capsule in *Vibrio vulnificus* Biotype-2 and its relationship to virulence for eels. *Infect Immun* 61: 1611–1618.
- Brinkman, A.B., Ettema, T.J.G., De Vos, W.M., and Van Der Oost, J. (2003) The Lrp family of transcriptional regulators. *Mol Microbiol* 48: 287–294.
- Callol, A., Pajuelo, D., Ebbesson, L., Teles, M., MacKenzie, S., and Amaro, C. (2015) Early steps in the European eel (*Anguilla Anguilla*)-*Vibrio vulnificus* interaction in the gills: role of the RtxA₁₃ toxin. *Fish Shell Imm* 43: 502–509.
- Carda-Diéguez, M., Ghai, R., Rodríguez-Valera, F., and Amaro, C. (2017) Wild eel microbiome reveals that skin mucus of fish could be a natural niche for aquatic mucosal pathogen evolution. *Microbiome* 5: 162.
- Casper-lindley, C., and Yildiz, F.H. (2014) VpsT is a transcriptional regulator required for expression of vps biosynthesis genes and the development of rugose colonial morphology in *Vibrio cholerae* O1 El tor. *J Bacteriol* 186: 1574–1578.
- Chung, H.Y., Kim, Y.T., Kim, S., Na, E.J., Ku, H.J., Lee, K. H., et al. (2016) Complete genome sequence of *Vibrio vulnificus* FORC-017 isolated from a patient with a hemorrhagic rash after consuming raw dotted gizzard shad. *Gut Pathog* 8: 4–9.
- Danin-Poleg, Y., Raz, N., Roig, F.J., Amaro, C., and Kashi, Y. (2015) Draft genome sequence of environmental bacterium *Vibrio vulnificus* CladeA-yb158. *Genome Announc* 3: 4–5.
- Felsenstein, J. (1985) Confidence limits on phylogenies: an approach using the bootstrap. *Evolution (N Y)* 39: 783–791.
- Fuangthong, M., Atichartpongkul, S., Mongkolsuk, S., and Helmann, J.D. (2001) OhrR is a repressor of ohrA, a key organic hydroperoxide resistance determinant in *Bacillus subtilis*. *J Bacteriol* 183: 4134–4141.
- Guindon, S., and Gascuel, O. (2003) A simple, fast and accurate algorithm to estimate large phylogenies by maximum likelihood. *Syst Biol* 52: 696–704.
- Hanahan, D. (1983) Studies on transformation of *Escherichia coli* with plasmids. *J Mol Biol* 166: 557–580.
- Hitchcock, P.J., and Brown, T.M. (1983) Morphological heterogeneity among *Salmonella* lipopolysaccharide chemotypes in silver-stained polyacrylamide gels. *J Bacteriol* 154: 269–277.
- Ho, Y.C., Hung, F.R., Weng, C.H., Li, W.T., Chuang, T.H., Liu, T.L., et al. (2017) Lrp, a global regulator, regulates the virulence of *Vibrio vulnificus*. *J Biomed Sci* 24: 54.
- Horseman, M.A., and Surani, S. (2011) A comprehensive review of *Vibrio vulnificus*: an important cause of severe sepsis and skin and soft-tissue infection. *Int J Infect Dis* 15: 157–166.
- Jeong, H.G., and Satchell, K.J.F. (2012) Additive function of *Vibrio vulnificus* MARTXVv and VvhA cytolysins promotes rapid growth and epithelial tissue necrosis during intestinal infection. *PLoS Pathog* 8: e1002581.
- Joseph, L.A., and Wright, A.C. (2004) Expression of *Vibrio vulnificus* capsular polysaccharide inhibits biofilm formation. *J Bacteriol* 186: 889–893.
- Jovanovic, G., Lloyd, L.J., Stumpf, M.P.H., Mayhew, A.J., and Buck, M. (2006) Induction and function of the phage shock protein extracytoplasmic stress response in *Escherichia coli*. *J Biol Chem* 281: 21147–21161.
- Juncker, A., and Willenbrock, H. (2003) Prediction of lipoprotein signal peptides in gram negative bacteria. *Protein Sci* 12: 1652–1662.
- Kim, Y.R., Lee, S.E., Kook, H., Yeom, J.A., Na, H.S., Kim, S. Y., et al. (2008) *Vibrio vulnificus* RTX toxin kills host cells only after contact of the bacteria with host cells. *Cell Microbiol* 10: 848–862.
- Kim, H.I., Wen, Y., Son, J.S., Lee, K.H., and Kim, K.S. (2013) The fur-iron complex modulates expression of the quorum-sensing master regulator, smcR, to control expression of virulence factors in *Vibrio vulnificus*. *Infect Immun* 81: 2888–2898.
- Krasteva, P.V., Jiunn, J.C., Shikuma, N.J., Beyhan, S., Navarro, M.V.A.S., Yildiz, F.H., and Sondermann, H. (2010) *Vibrio cholerae* vpsT regulates matrix production and motility by directly sensing cyclic di-GMP. *Science* 327: 866–868.
- Kumar, S., Stecher, G., and Tamura, K. (2016) MEGA7: molecular evolutionary genetics analysis version 7.0 for bigger datasets. *Mol Biol Evol* 33: 1870–1874.
- Lee, C.T., Amaro, C., Wu, K.M., Valiente, E., Chang, Y.F., Tsai, S.F., et al. (2008) A common virulence plasmid in biotype 2 *Vibrio vulnificus* and its dissemination aided by a conjugal plasmid. *J Bacteriol* 190: 1638–1648.
- Lee, S.H., Angelichio, M.J., Mekalanos, J.J., and Camilli, A. (1998) Nucleotide sequence and spatiotemporal expression of the *Vibrio cholerae* vieSAB genes during infection. *J Bacteriol* 180: 2298–2305.
- Lee, C.T., Pajuelo, D., Llorens, A., Chen, Y.H., Leiro, J.M., Padrós, F., et al. (2013) MARTX of *Vibrio vulnificus* biotype 2 is a virulence and survival factor. *Environ Microbiol* 15: 419–432.
- Liu, M.I., Rose, M., and Crosa, J.H. (2011) Homodimerization and binding of specific domains to the target DNA are essential requirements for HlyU to regulate expression of the virulence gene rtxA1, encoding the repeat-in-toxin protein in the human pathogen *Vibrio vulnificus*. *J Bacteriol* 193: 6895–6901.

- Livak, K.J., and Schmittgen, T.D. (2001) Analysis of relative gene expression data using real-time quantitative PCR and the 2- $\Delta\Delta$ CT method. *Methods* 25: 402–408.
- Madan Babu, M., and Sankaran, K. (2002) DOLOP - database of bacterial lipoproteins. *Bioinformatics* 18: 641–643.
- Manganelli, R., and Gennaro, M.L. (2017) Protecting from envelope stress: variations on the phage-shock-protein theme. *Trends Microbiol* 25: 205–216.
- Masatoshi, N., and Kumar, S. (2000) *Molecular Evolution and Phylogenetics*. Oxford: Oxford University Press.
- Mathur, J., Davis, B.M., and Waldor, M.K. (2007) Antimicrobial peptides activate the *Vibrio cholerae* σ E regulon through an OmpU-dependent signalling pathway. *Mol Microbiol* 63: 848–858.
- Mathur, J., and Waldor, M.K. (2004) The *Vibrio cholerae* ToxR-regulated porin OmpU confers resistance to antimicrobial peptides. *Infect Immun* 72: 3577–3583.
- Meibom, K.L., Blokesch, M., Dolganov, N.A., Wu, C.Y., and Schoolnik, G.K. (2005) Microbiology: chitin induces natural competence in *Vibrio cholerae*. *Science* 310: 1824–1827.
- Metzger, L.C., and Blokesch, M. (2016) Regulation of competence-mediated horizontal gene transfer in the natural habitat of *Vibrio cholerae*. *Curr Opin Microbiol* 30: 1–7.
- Miller, J.H. (1972) *Experiments in Molecular Genetics*. Cold Spring Harbor, NY: Cold Spring Harbor Laboratory Press.
- Mitchell, S.L., Ismail, A.M., Kenrick, S.A., and Camilli, A. (2015) The VieB auxiliary protein negatively regulates the VieSA signal transduction system in *Vibrio cholerae* Ssgnaling and cellular microbiology. *BMC Microbiol* 15: 1–16.
- Murciano, C., Lee, C.T., Fernández-Bravo, A., Hsieh, T.H., Fouz, B., Hor, L.I., and Amaro, C. (2017) MARTX toxin in the zoonotic serovar of *Vibrio vulnificus* triggers an early cytokine storm in mice. *Front Cell Infect Microbiol* 7: 1–19.
- Nieckarz, M., Raczowska, A., Jaworska, K., Stefanska, E., Skorek, K., Stosio, D., and Brzostek, K. (2017) The role of OmpR in the expression of genes of the KdgR regulon involved in the uptake and depolymerization of oligogalacturonides in *Yersinia enterocolitica*. *Front Cell Infect Microbiol* 7: 1–25.
- Oliver, J.D. (2015) The biology of *Vibrio vulnificus*. *Microbiol Spectr* 3: 1–10.
- Pajuelo, D., Hernández-Cabanyero, C., Sanjuán, E., Lee, C. T., Silva-Hernández, F.X., Hor, L.I., et al. (2016) Iron and fur in the life cycle of the zoonotic pathogen *Vibrio vulnificus*. *Environ Microbiol* 18: 4005–4022.
- Pajuelo, D., Lee, C.T., Roig, F.J., Hor, L.I., and Amaro, C. (2015) Novel host-specific iron acquisition system in the zoonotic pathogen *Vibrio vulnificus*. *Environ Microbiol* 17: 2076–2089.
- Phadtare, S., and Severinov, K. (2010) RNA remodeling and gene regulation by cold shock proteins. *RNA Biol* 7: 788–795.
- Philippe, N., Alcaraz, J.P., Coursange, E., Geiselmann, J., and Schneider, D. (2004) Improvement of pCVD442, a suicide plasmid for gene allele exchange in bacteria. *Plasmid* 51: 246–255.
- Posada, D. (2008) jModelTest: Phylogenetic model averaging. *Mol Biol Evol* 25: 1253–1256.
- Reed, L.J., and Muench, H. (1938) A simple method of estimating fifty percent endpoints. *Am J Epidemiol* 27: 493–497.
- Rodionov, D.A., Dubchak, I.L., Arkin, A.P., Alm, E.J., and Gelfand, M.S. (2005) Dissimilatory metabolism of nitrogen oxides in bacteria: comparative reconstruction of transcriptional networks. *PLoS Comput Biol* 1: 0415–0431.
- Rodionov, D.A., Mironov, A.A., Rakhmaninova, A.B., and Gelfand, M.S. (2000) Transcriptional regulation of transport and utilization systems for hexuronides, hexuronates and hexonates in gamma purple bacteria. *Mol Microbiol* 38: 673–683.
- Roig, F.J., González-Candelas, F., Sanjuán, E., Fouz, B., Feil, E.J., Llorens, C., et al. (2018) Phylogeny of *Vibrio vulnificus* from the analysis of the core-genome: implications for intra-species taxonomy. *Front Microbiol* 8: 1–13.
- Sanjuán, E., and Amaro, C. (2004) Protocol for specific isolation of virulent strains of *Vibrio vulnificus* serovar-E (biotype 2) from environmental samples. *Appl Environ Microbiol* 70: 7024–7032.
- Sanjuán, E., González-Candelas, F., and Amaro, C. (2011) Polyphyletic origin of *Vibrio vulnificus* biotype 2 as revealed by sequence-based analysis. *Appl Environ Microbiol* 77: 688–695.
- Satchell, K.J.F. (2011) Structure and function of MARTX toxins and other large repetitive RTX proteins. *Annu Rev Microbiol* 65: 71–90.
- Shao, C.P., Lo, H.R., Lin, J.H., and Hor, L.I. (2011) Regulation of cytotoxicity by quorum-sensing signaling in *Vibrio vulnificus* is mediated by SmcR, a repressor of hlyU. *J Bacteriol* 193: 2557–2565.
- Sunyer, O., and Tort, L. (1995) Natural hemolytic and bactericidal activities of sea bream *Sparus aurata* serum are affected by the alternative complement pathway. *Vet Immunol Immunopathol* 2427: 333–345.
- Tamura, K. (1992) Estimation of the number of nucleotide substitutions when there are strong transition-transversion and G+C-content biases. *Mol Biol Evol* 6: 678–687.
- Weigel, W.A., and Demuth, D.R. (2016) QseBC, a twocomponent bacterial adrenergic receptor and global regulator of virulence in Enterobacteriaceae and Pasteurellaceae. *Mol Oral Microbiol* 31: 379–397.
- Weigel, W.A., Demuth, D.R., Torres-Escobar, A., and Juárez-Rodríguez, M.D. (2015) *Aggregatibacter actinomycetemcomitans* QseBC is activated by catecholamines and iron and regulates genes encoding proteins associated with anaerobic respiration and metabolism. *Mol Oral Microbiol* 30: 384–398.
- Wright, A.C., and Morris, J.G. (1991) The extracellular cytolysin of *Vibrio vulnificus*: inactivation and relationship to virulence in mice. *Infect Immun* 59: 192–198.
- Yamamoto, K., Wright, A.C., Kaper, J.B., and Morris, J.G. (1990) The cytolysin gene of *Vibrio vulnificus*: sequence and relationship to the *Vibrio cholerae* El tor hemolysin gene. *Infect Immun* 58: 2706–2709.

Table 1. Selected differentially expressed genes in eel serum vs CM9.

Gene(s) ^a	Fc ^b	Iron stimulon	Fur regulon	Putative function/process ^c
Metabolic regulators and sensors				
<i>cytR</i>	14.3	No	Yes	Repressor (response to nucleoside starvation, competence) (Antonova <i>et al.</i> , 2012)
<i>arcA</i>	3.5	No	Yes	Repressor for aerobic metabolism
Cyn operon transcriptional activator	3	No	Yes	Activator of cyanide metabolism, a subproduct from urea
<i>fabR</i>	-2.5	Yes	Yes	Repressor for unsaturated fatty acid biosynthesis
<i>fur</i>	-2.3	No	Yes	Regulator of iron-uptake mainly acting as a repressor
<i>aer</i>	-2.7	No	Yes	Aerotaxis sensor receptor protein
<i>phoR, phoB</i>	-(2.7-3.8)	Yes	No/Yes	PhoR (histidine kinase/phosphatase for PhoB) and PhoB (positive transcriptional factor for Pho regulon) involved in phosphate starvation
Nitrogen regulatory protein P-II	-6.8	Yes	Yes	Nitrogen starvation
<i>kdgR</i>	-8.2	Yes	Yes	Repressor for oligogalacturonide metabolism (Nieckarz <i>et al.</i> , 2017)
<i>uxuR</i>	-9.4	Yes	Yes	Repressor for oligoglucuronide metabolism (Rodionov <i>et al.</i> , 2000)
<i>fruR (cra)</i>	-89.1	Yes	Yes	Catabolite repressor/activator (Cra) protein
Anaerobic respiration				
Nitrate reductase cytochrome c550-type subunit	13	Yes	No	Nitrate reductase complex subunit
<i>napA, napC, napD, napF, napG, napH</i>	3.7-11.4	Some	Some	Subunits of the periplasmic nitrate reductase,
<i>ccoN</i>	11	No	Yes	Cytochrome c oxidase subunit
<i>nrfBCD</i>	4.6-5.9	No	No	Formate-dependent nitrite reductase complex
Peptide/amino acid/ammonium metabolism (including transporters)				
<i>nupC</i>	13.7	Yes	Yes	Permease for nucleoside uptake
<i>rbsBD</i>	4.2-8.9	No	No	Ribose ABC transport system
PTS system, N-acetylglucosamine-specific IIB component	8.7	Yes	No	Aminosugar transport
Serine transporter	7.6	Yes	No	Aminoacid transport
Tail-specific protease precursor	3.5	Yes	Yes	Protein degradation
Peptide ABC transporters	4.2-2.2	No	Yes	Peptide transport
N-Acetyl-D-glucosamine ABC transport system	2.2	No	No	Aminosugar transport
Glutamine synthetase type I	2.3	No	Yes	Ammonia assimilation cycle
ABC transporter, periplasmic spermidine putrescine-binding protein PotD	2	Yes	Yes	Polyamine transport
Iron uptake				
Vulnibactin biosynthetic genes	8.4-2	Yes	Yes	Vulnibactin biosynthesis and transport
Heme/Hemin transport	5.4-3.1	Yes	Yes	Heme/Hemin transport and utilization
Ferric iron ABC transporters	4.3-2.7	Yes	Yes	Ferric iron transport
Aerobactin transport	3-2	Yes	Yes	Aerobactin transport
<i>ftbp (or vep20)</i>	3	Yes	No	Eel transferrin binding (Pajuelo <i>et al.</i> , 2015)
Stress protection related genes				
Anaerobic glycerol-3-phosphate dehydrogenase subunits (A, B, C)	22-33	No	No	Phospholipid biosynthesis/membrane regeneration
Glycerophosphoryl diester phosphodiesterase	24.8	No	No	Phospholipid biosynthesis/membrane regeneration
Glycerol kinase	24.3	No	Yes	Phospholipid biosynthesis/membrane regeneration
<i>hcp</i>	13.8	No	No	Hydroxylamine reductase, a putative scavenger of potentially toxic by-products of nitrate metabolism
Alkyl hydroperoxide reductase subunit C-like protein	10.3	Yes	Yes	Resistance to oxidative stress
<i>cspE, cspG</i>	6.3-8.5	Yes	Yes	Cold shock proteins recently involved in stress caused by membrane damage
Formate efflux transporter	6	Yes	Yes	Resistance to microcidal peptides
<i>madN</i>	6	No	Yes	Resistance to microcidal peptides
<i>usp8</i>	5.3	No	Yes	Universal stress protein family 8 related to resistance to oxidative stress

(Continues)

Table 1. Continued

Gene(s) ^a	Fc ^b	Iron stimulon	Fur regulon	Putative function/process ^c
1-acyl-sn-glycerol-3-phosphate acyltransferase	4.9	No	No	Phospholipids biosynthesis/membrane regeneration
Thiol peroxidase, Bcp-type	4.7	Yes	Yes	Resistance to oxidative stress
<i>plsX</i>	4.2	No	Yes	Phosphate: acyl-ACP acyltransferase involved in phospholipid biosynthesis/membrane regeneration
Glutathione synthetase	3.8	No	No	Resistance to oxidative stress
<i>pspABC</i>	2.6–3.5	No	Some	Phage shock proteins involved in resistance to different stresses (Manganelli and Gennaro, 2017)
Cold-shock DEAD-box protein A (helicase of RNA)	3.1	No	Yes	Resistance to different stresses
Isopentenyl-diphosphate delta-isomerase	3	No	No	Phospholipids biosynthesis/membrane regeneration
<i>norR</i>	2.8	No	No	Anaerobic nitric oxide reductase transcription regulator
<i>dndDE</i>	2	No	Yes	DNA phosphorothioate modification, a process that seems to protect DNA from both H ₂ O ₂ and hydroxyl radicals <i>in vivo</i>
Cardiolipin synthetase	2.1	No/Yes	Yes	Phospholipids biosynthesis/membrane regeneration
<i>ompU</i>	2	Yes	Yes	Resistance to microcidal peptides (Mathur <i>et al.</i> , 2007)
<i>rseABC</i>	–(2.6–5.4)	Yes	Some	Negative regulatory proteins for RpoE, a sigma factor for envelope stress response
Organic hydroperoxide resistance transcriptional regulator <i>ohr</i>	–2.9	No	Yes	Repressor for organic hydroperoxide resistance
<i>rpoD</i>	–7	No	No	Nitric oxide-sensitive repressor of genes involved in protecting the cell against nitrosative stress
<i>nsrR</i>	–7.2	Yes	Yes	Repressor for resistance to nitrosative stress
Flagellum and pili				
MSHA cluster	4.8–2.8	Some	Some	Pili MSHA biosynthesis
<i>flaDEF</i>	–(2–3.9)	Some	Yes	Flagellin proteins
<i>fljL</i>	–2.2	Yes	Yes	Controls the rotational direction of flagella during chemotaxis
<i>fljS</i>	–2.2	Yes	Yes	Flagellar secretion chaperone
<i>flgABCDE, flgG</i>	–(2.4–5)	Some	Some	Flagellar basal-body rod proteins
<i>flhF</i>	–2.5	Yes	Yes	Flagellar biosynthesis protein
<i>flhN</i>	–4.9	Yes	Yes	Flagellar synthesis regulator
RNA polymerase sigma factor for flagellar operon	–4.9	Yes	Yes	Flagellar biosynthesis
<i>motX</i>	–5.2	Yes	Yes	Sodium-type polar flagellar protein
<i>flgN</i>	–6.1	No	Yes	Flagellar biosynthesis protein
<i>flgM</i>	–6.7	Yes	Yes	Hook associated protein
<i>motA</i>	–12.1	Yes	Yes	Flagellar motor rotation protein
LPS and capsule				
<i>rffC, wzbc, waaL, rfbD</i>	4.2–2.1	Yes	Yes	LPS biosynthesis
<i>wza, lptB</i>	2.3	No	Yes	LPS biosynthesis
<i>yciS</i>	–3.8	Yes	Yes	LPS (core) biosynthesis and assembly
<i>cpsC</i>	–2	No	Yes	Capsule biosynthesis
<i>sypO</i>	–2.9	Yes	Yes	Capsule biosynthesis
SOS response, DNA repair and competence				
<i>tfoX</i>	3.1	Yes	Yes	Positive regulator of competence
<i>uvrC</i>	2.2	Yes	No	Excinuclease ABC subunit C for DNA repair
<i>lexA</i>	–3.1	No	Yes	Repressor of SOS response
<i>dns</i>	–5.8	Yes	Yes	Competence related: degradation of DNA for nutrient uptake
Virulence factors and related regulators				
<i>vvhAB</i>	31–118	Yes	No	Haemolysin (vulnificolysin) and transport protein
<i>rtxA1</i>	–2.6	No	No	Toxin involved in cytokine storm in mice (Murciano <i>et al.</i> , 2017)

(Continues)

Table 1. Continued

Gene(s) ^a	Fc ^b	Iron stimulon	Fur regulon	Putative function/process ^c
<i>rtxC</i>	-5	No	Yes	Cytolysin-activating lysine-acyltransferase, <i>rtxA1</i> activator
<i>lrp</i>	2.4	Yes	Yes	Global regulator involved in virulence that is upregulated under nutrient starvation (Ho <i>et al.</i> , 2017)
<i>smcR</i>	2	No	Yes	Master regulator of <i>quorum sensing</i> . It downregulates <i>hlyU</i> (Kim <i>et al.</i> , 2013)
<i>luxU</i>	-2	Yes	Yes	Phosphorelay protein LuxU involved in <i>quorum sensing</i>
<i>luxO</i>	-3	Yes	Yes	Indirectly represses <i>smcR</i> transcription
<i>csrA</i>	-3	Yes	Yes	Carbon storage regulator, a global repressor of multiple virulence factors
<i>hlyU</i>	-4.6	No	Yes	<i>rtxA1</i> activator
DNA-binding protein H-NS	-10.2	Yes	Yes	DNA-binding protein implicated in transcriptional repression (silencing) of mobile genetic element transcription

a. Identified differentially expressed genes are indicated.

b. Fc: fold-change value or range of fold-change values for each individual gene or for a group of related genes respectively. See Supporting Information Table S2 for specific gene and fold-change value.

c. Putative function for the gene and related process.

Table 2. Selected differentially expressed genes in human serum vs CM9.

Gene(s) ^a	Fc ^b	Iron stimulon	Fur regulon	Putative function/process ^c
Protection against oxidative stress				
Manganese superoxide dismutase	9.4	Yes	Yes	Oxidative stress
S-(hydroxymethyl)glutathione dehydrogenase)	5.6	No	No	Oxidative stress
Glutathione peroxidase	3.16	Yes	Yes	Oxidative stress
<i>dndD</i>	2.9	No	Yes	DNA sulphur modification
Metabolism				
<i>fruR</i>	-8	Yes	Yes	Catabolite repressor/activator (Cra) protein
Iron uptake				
Vulnibactin biosynthetic genes	34.4-4.3	Yes	Yes	Vulnibactin biosynthesis and transport
Flagellum and pili				
MSHA cluster	8.9-3.5	Some	Some	Pili MSHA biosynthesis
<i>figF</i>	-3.1	No	Yes	Flagellar basal-body rod protein
<i>flaEF</i>	-(3.7-4.7)	Yes/No	Yes	Flagellin proteins
<i>matY</i>	-4.2	Yes	Yes	Sodium-type flagellar protein
<i>matX</i>	-5.1	Yes	Yes	Sodium-type polar flagellar protein
<i>matA</i>	-8.7	Yes	Yes	Flagellar motor rotation protein

a. Identified differentially expressed genes are indicated.

b. Fc: fold-change value or fold-change range for each individual identified gene or for a group of related genes respectively. See Supporting Information Table S3 for specific gene and value.

c. Putative function for the gene and related process.

Table 3. Selected differentially expressed genes in iron-overloaded human serum vs CM9.

Gene(s) ^a	Fc ^b	Iron stimulon	Fur regulon	Putative function/process ^c
Metabolic regulators				
<i>fabR</i>	-2.4	Yes	Yes	Repressor for unsaturated fatty acid biosynthesis
<i>trpR</i>	-4	Yes	Yes	Aminoacid (Trp) biosynthesis
<i>metJ</i>	-4.4	No	Yes	Aminoacid (Met) biosynthesis (repressor)
<i>yvoA</i>	-4.5	No	No	2-aminoethylphosphonate uptake and metabolism regulator (phosphonate metabolism)
<i>kdgR</i>	-6.2	Yes	Yes	Repressor for aminosugars metabolism (Nieckarz <i>et al.</i> , 2017)
Metabolic and nutrient transport genes (including iron)				
<i>nirB</i>	63.5	No	Yes	Assimilatory nitrite reductase
<i>malQ</i>	44.9	No	Yes	4-alpha-glucanotransferase (amylomaltase)
Nitrate ABC transporter, nitrate-binding protein	22.2	No	No	Nitrogen metabolism
<i>malK</i> , <i>malG</i> , <i>mall</i>	19.4-3.8	No	Yes	Maltose/maltodextrin ABC transporter
<i>glgB</i> , <i>glgX</i>	6.4-15.3	No	Yes	Glycogen branching and debranching enzymes
Amine oxidase, flavin-containing	11.6	No	Yes	Nitrogen metabolism
<i>amtB</i>	11	No	No	Ammonium transporter
<i>dctM</i> , <i>dctQ</i>	6.5-5.4	No	No	TRAP dicarboxylate transporters
<i>murP</i>	6.4	No	No	Aminosugar transport (PST system)
ABC-type phosphate transport system	5.7	No	No	Phosphate transport
<i>artI</i> , <i>artQ</i>	5.5-3.1	No	No	Arginine ABC transporters
C4-dicarboxylate like transporter	5	No	No	Dicarboxylate transport
<i>sapB</i>	4.7	No	Yes	Peptide transport system permease
Predicted ferric reductase	4.1	No	Yes	Ferric reductase
N-Acetyl-D-glucosamine ABC transport system	3.6	No	No	Aminosugar transport
<i>vuuA</i>	-5	Yes	Yes	Ferric vulnibactin receptor
Stress protection related genes				
<i>pspABC</i>	69-59	No	Some	Phage shock proteins involved in resistance to different stresses
Phosphoglycerol transferase I	27.2	Yes	Yes	Phospholipid biosynthesis/membrane regeneration
Anaerobic glycerol-3-phosphate dehydrogenase subunits (B, C)	10-8	No	No	Phospholipid biosynthesis/membrane regeneration
S-(hydroxymethyl)glutathione dehydrogenase	9	No	No	Peroxislipid detoxification
Glutathione S-transferase	8.9	No	Yes	Peroxislipid detoxification
Thiol peroxidase, Bcp-type	4.4	Yes	Yes	Resistance to oxidative stress
Glutathione synthetase	3.8	No	No	Resistance to oxidative stress
<i>msrA</i>	3.8	No	No	Peptide methionine sulfoxide reductase involved in reparation of oxidized proteins
YfgC precursor	3.8	Yes	Yes	Outer membrane integrity
<i>degQ</i> , <i>degS</i>	3.3-2.7	No/Yes	No	Outer membrane integrity
<i>cspA</i> , <i>cspE</i>	2.6	Yes	Yes/No	Cold shock proteins involved in resistance to different stresses
Flagellum and pili				
<i>rpoN</i>	7.6	Yes	No	RNA polymerase sigma factor
<i>mshE</i> , <i>mshJ</i> , <i>mshQ</i>	4.5-2.8	No	Some	Pili MSHA
Von Willebrand factor type A domain protein	4.2	No	No	Pili MSHA
<i>flhH</i> , <i>flhMNO</i>	3.6-2.6	Some	Some	Flagellar biosynthesis proteins
<i>flgF</i> , <i>flgJ</i> , <i>flgT</i>	2.6-2	Some	Some	Flagellar proteins
Probable type IV pilus assembly FimV-related	2.8	No	No	Pili MSHA
LPS and capsule				
O-antigen acetylase	10.2	No	Yes	LPS modification
<i>sypJP</i>	3.3-5.3	No	No	Capsule biosynthesis
<i>cpsD</i>	3.8	No	No	Capsule biosynthesis
Virulence factors and related regulators				
<i>qseB</i>	11.5	No	No	Positive regulation of flagella and motility
<i>ktrB</i>	6.2	No	No	Potassium uptake protein involved in serum resistance
<i>rtxA1</i>	6.1	No	No	Toxin involved in cytokine storm in mice (Murciano <i>et al.</i> , 2017)
<i>vvhA</i>	4.2	Yes	No	Haemolysin (vulnificolysin)

(Continues)

Table 3. Continued

Gene(s) ^a	Fc ^b	Iron stimulon	Fur regulon	Putative function/process ^c
<i>ompR</i>	3.1	No	Yes	Virulence regulator that responds to osmotic pressure
RTX toxin transporter	2.3	No	Yes	MARTX transporter
<i>hlyU</i>	2	No	Yes	<i>rtxA1</i> activator
<i>vpsT</i>	-4	Yes	No	Repressor of biofilm and biofilm related polysaccharide formation (Krsteva <i>et al.</i> , 2010)
<i>vieB</i>	-4.3	No	Yes	Controls VieA that activates virulence genes (Mitchell <i>et al.</i> , 2015)
<i>fleN</i>	-4.3	No	No	Repressor of flagellum biosynthesis
<i>smcR</i>	-6.2	No	No	Master regulator of <i>quorum sensing</i> . It downregulates <i>hlyU</i> (Kim <i>et al.</i> , 2013)

a. Identified differentially expressed genes are indicated.

b. Fc: fold-change value or fold-change range for each individual identified gene or for a group of related genes respectively. See Supporting Information Table S4 for specific gene and value.

c. Putative function for the gene and related process.

Table 4. Comparison of fold-change values obtained by array and RT-qPCR with the *V. vulnificus* R99 strain. In case of RT-qPCR, results were obtained using *recA* as the reference gene and the fold induction ($2^{-\Delta\Delta Ct}$) for each gene was calculated.

Sample ^a	Gene for	Fold change ^b		
		Array	RT-qPCR	
ES vs CM9	Cold shock protein CspE	8.49 (+)	2.51 (+)	
	dTDP-4-dehydrorhamnose 3,5-epimerase	2.47 (+)	1.26 (=)	
	RtxA	-2.62 (-)	-7.03 (-)	
	VvhA	30.92 (+++)	6.36 (+)	
	VvhB	118.28 (+++)	5.21 (+)	
	CpsC	-1.59 (=)	-5.62 (-)	
	Vep07	5.67 (+)	7.29 (+)	
	3-deoxy-D-manno-octulosonate 8-phosphate phosphatase KsdC	-2.25 (-)	-0.71 (=)	
	Acyl-[acyl-carrier-protein]-UDP-N-acetylglucosamine O-acyltransferase LpxA	2.09 (+)	2.88 (+)	
	UDP-3-O-[3-hydroxymyristoyl] glucosamine N-acyltransferase LpxD	NP	2.57 (+)	
	Tetraacyldisaccharide 4'-kinase LpxK	NP	2.72 (+)	
	Lipid A core-O-antigen ligase WaaL	2.44 (+)	4.95 (+)	
	OmpU	1.97 (=)	2.31 (+)	
	HlyU	-4.64 (-)	-2.89 (-)	
	HS vs CM9	NADPH:quinone reductase	1.92 (=)	1.51 (=)
		RtxA	NP	-0.72 (=)
		VvhA	NP	2.47 (+)
Acyl-[acyl-carrier-protein]-UDP-N-acetylglucosamine O-acyltransferase LpxA		NP	1.01 (=)	
UDP-3-O-[3-hydroxymyristoyl] glucosamine N-acyltransferase LpxD		NP	1.09 (=)	
Tetraacyldisaccharide 4'-kinase LpxK		NP	1.73 (+)	
Lipid A core-O-antigen ligase WaaL		NP	2.43 (+)	
Glycosyltransferase SypJ		NP	3.67 (+)	
HS+Fe vs CM9	Glycogen phosphorylase	27.5 (+++)	2.73 (+)	
	RtxA	6.08 (+)	40.79 (+++)	
	VvhA	4.16 (+)	4.28 (+)	
	VvhB	NP	-4.79 (-)	
	Glycosyltransferase SypJ	5.32 (+)	3.13 (+)	
	Capsular polysaccharide synthesis enzyme CpsD, exopolysaccharide synthesis	3.75 (+)	8.73 (+)	
	Potassium uptake protein, integral membrane component ktrB	6.18 (+)	3.16 (+)	
	Maltose/maltodextrin ABC transporter, permease protein MalG	3.80 (+)	10.32 (++)	
	VieB	-4.26 (-)	-1.95 (=)	
	OseB	11.46 (++)	3.59 (+)	
	HlyU	2 (+)	1.83 (=)	
	CpsA	-5.57 (-)	-5.92 (-)	
	CpsB	NP	5.14 (+)	
	CpsH	NP	3.48 (+)	
	FUR	NP	5.12 (+)	
FruR	NP	2.88 (+)		

a. RNA samples were obtained from 6 h cultures in CM9, ES (eel serum), HS (human serum) and HS+Fe (iron-overloaded human serum) by using the Direct-zol™ RNA Miniprep kit (Zymo), TURBO™ DNase (Ambion) and RNA Clean & Concentrator™ Kit (Zymo).

b. Qualitative classification: =, $-2 < X < 2$; +, $2 \leq X < 10$; ++, $10 \leq X < 25$; +++, $25 \leq X$; -, $-10 < X \leq -2$; --, $-25 < X \leq -10$; ---, $X \leq -25$. NP: there was not detected as differentially expressed by microarray hybridization.

Table 5. Virulence and resistance of strain R99 and its derivative mutants to innate immunity in blood.

Strains	Virulence ^a			Resistance to innate immunity in blood ^b				
	Eel		Mice	Eel			Human	
	intra-peritoneal	immersion	intra-peritoneal	Blood	Blood Phagocytes	Serum	Blood	Serum
R99	1.7 × 10 ^b	2 × 10 ⁶	4 × 10 ⁵	+++	+	+++	±	±
Δ <i>vep07</i>	5.2 × 10 ^{5*}	>10 ^{6*}	6 × 10 ⁵	+	±*	+	±	±
<i>cvep07</i>	1.4 × 10 ^b	6 × 10 ⁶	7 × 10 ⁵	+++	+	+++	±	±
Δ <i>vep07</i> Δ <i>ftbp</i>	>10 ⁷	>10 ⁷	6 × 10 ⁵	-*	NT	-*	±	±
Δ <i>ftbp</i>	1 × 10 ⁶	>10 ^{6*}	NT	+	NT	±*	NT	NT
Δ <i>vvhA</i>	3.3 × 10 ^b	1.4 × 10 ⁷	NT	+++	NT	+++	NT	NT

a. Virulence was expressed as LD₅₀ in CFU per fish/mouse in case of intra-peritoneal injection and CFU ml⁻¹ in case of bath infection (Amaro *et al.*, 1995). Mice (6- to 8-week-old female BALB/c mice, Charles River, France) and farmed eels (European eel *Anguilla anguilla*, purchased from a local eel-farm that does not vaccinate against *V. vulnificus*).

b. Resistance to innate immunity in blood was measured as the ratio between bacterial counts at 4 h and 0 h of incubation in blood, phagocyte suspension and serum (SI_{4h}): -, no survival; ±, 0 < SI_{4h} < 1; +, 1 < SI_{4h} < 10; ++, 10 < SI_{4h} < 25; +++ > 25.

NT, non tested.

Asterisk (*) denotes significant differences in survival index after 4 h of incubation SI_{4h} (p < 0.01) between R99 and the derivative mutants.

Table 6. Resistance to human and eel serum of strain R99 and its derivative mutants: effect of iron and complement inactivation.

Strains	Human serum ^a			Eel plasma ^a				
	Fresh	Iron overload ²	Complement inactivation ^b	Fresh	Iron overload ²	Complement inactivation ^b		
						All pathways	Alternative-lectin pathway	Classical pathway
R99	±	+	+	+++	+++	+++	+++	+++
<i>Δvep07</i>	±	+	+	+*	+*	+++	+++	+*
<i>cvep07</i>	±	+	+	+++	+++	+++	+++	+++
<i>Δvep07Δftbp</i>	±	+	+	-	-	+*	±*	±*
<i>Δftbp</i>	±	+	+	+*	+++	+*	+*	+*

a. Resistance to innate immunity in blood was measured as the ratio between bacterial counts at 4 h and 0 h of incubation in blood, phagocyte suspension and plasma/serum (SI_{4h}): -, no survival; ±, $0 < SI_{4h} < 1$; +, $1 < SI_{4h} < 10$; ++, $10 < SI_{4h} < 25$; +++ > 25.

b. Iron-overloaded serum was obtained by adding 100 μ M $FeCl_3$ to fresh serum. Complement activity was completely abolished by heating eel and human-serum at 56°C for 30 min and 1 h respectively. Alternative-lectin pathway was inactivated by heating at 47°C 20 min and classical pathway by incubating with EGTA- $MgCl_2$ (Sunyer and Tort, 1995; Amaro *et al.*, 1997).

NT, non tested.

Asterisk (*) represents significant differences in SI_{4h} ($p < 0.001$) between the derivative mutants and the R99 strain.

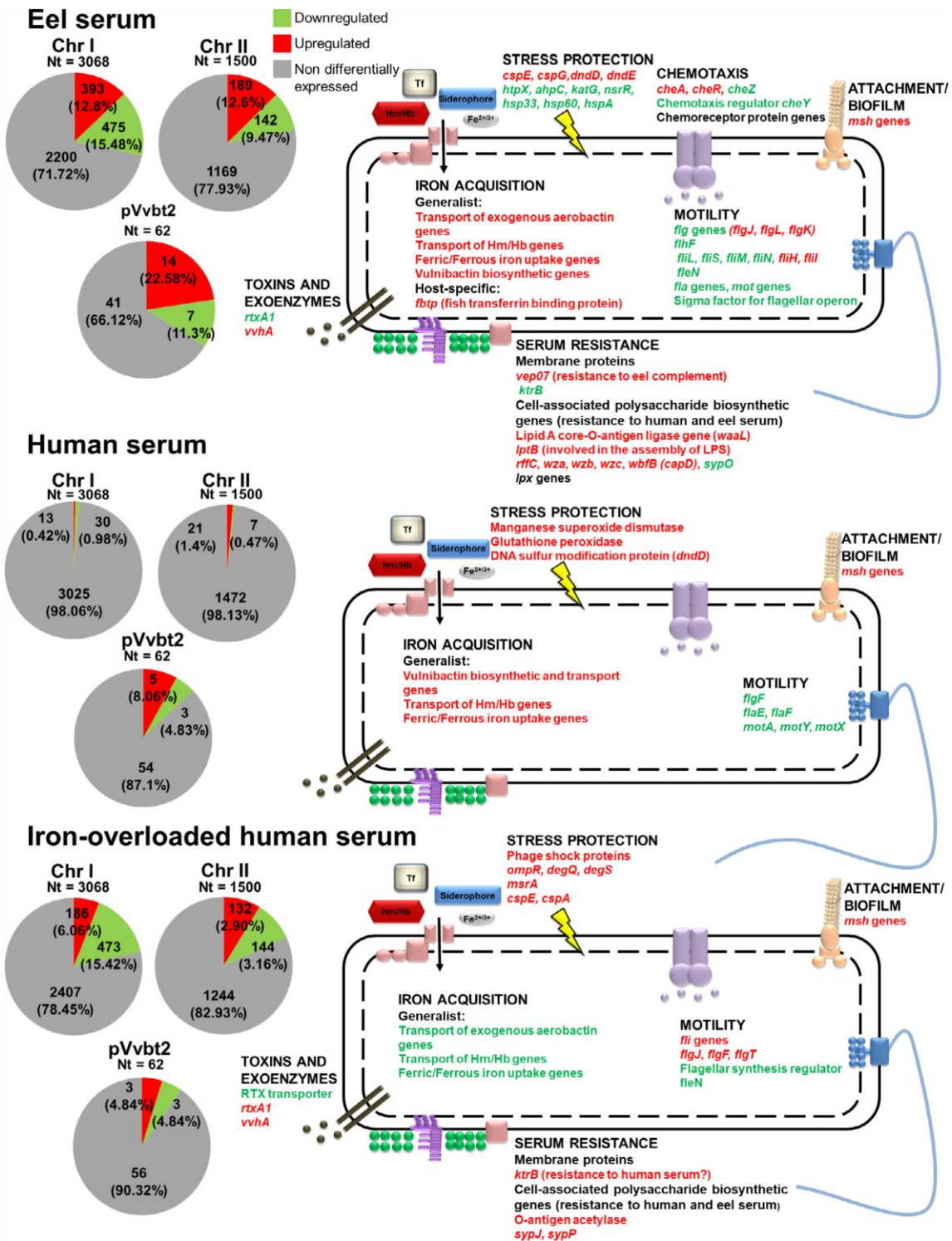


Fig. 1. Differentially expressed genes by *V. vulnificus* R99 strain in serum vs a minimal medium (CM9). Genes that exhibited a value of fold-change $-2 \leq X \leq 2$ with a p-value cut-off of 0.05 (averages from three independent biological samples) were considered as differentially expressed genes. Left: distribution of the differentially expressed genes per regulation category (upregulated, downregulated or nonregulated) and replicon (two chromosomes and one plasmid). The categories are represented as a colour code. Right: main differentially affected virulence- and survival-related processes according to Pajuelo et al. (2016). Red colour: upregulated genes; Green colour: downregulated genes; Black colour: a group of related genes for the same biological process, some upregulated and other downregulated.

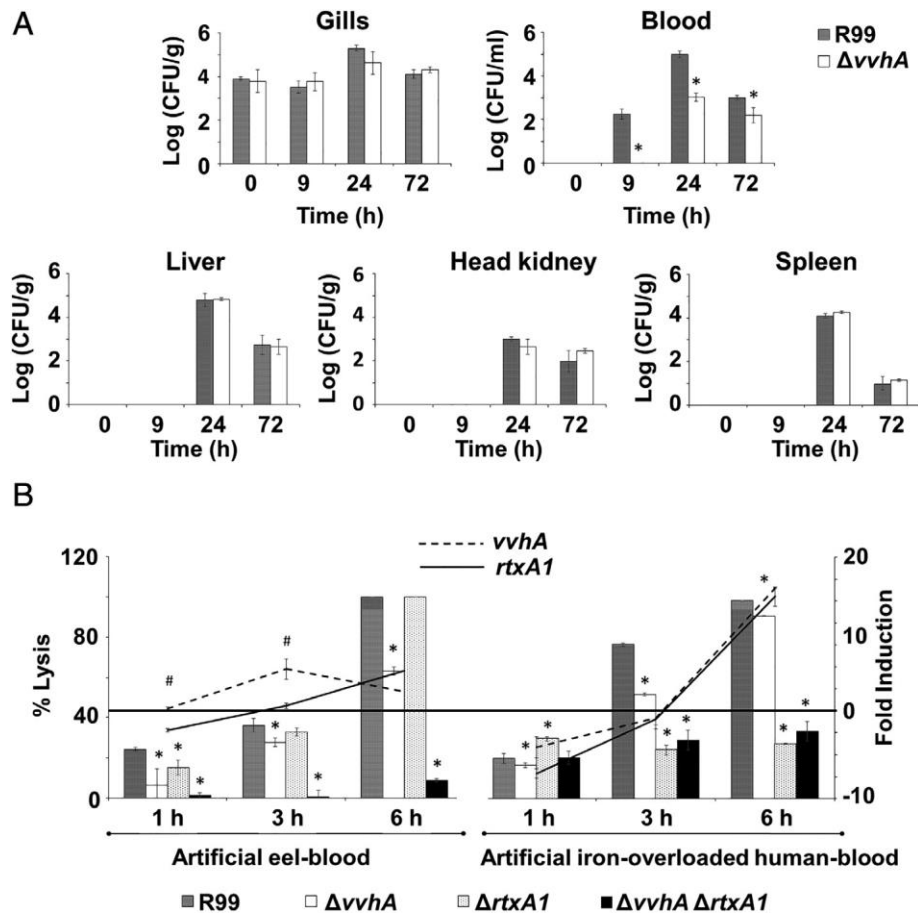


Fig. 2. Role of *vvhA* in eel colonization and haemolysis. A. *Eel colonization and invasion.* Groups of 24 eels per strain (three animals per sampling point) were infected by immersion with either R99 strain or the mutant strain ($\Delta vvhA$) at the same dose (2×10^6 CFU ml⁻¹) and gills, blood, liver, head kidney and spleen were sampled for bacterial counting on TSA-1 (1% NaCl) at 0, 9, 24 and 72 h post-infection. Results are presented as average (\pm standard error) of three independent biological experiments (three sampled animals per experiment, sampling time and organ). *Significant differences in bacterial counts from R99 vs $\Delta vvhA$ infected eels using the unpaired Student's *t*-test ($p < 0.05$). B. *Haemolysis and gene expression in artificial blood.* Artificial eel and human (iron-overloaded) blood were prepared by adding erythrocytes to their respective sera (10^6 cells ml⁻¹). Then, artificial blood samples were infected with either R99 or each one of its derivative mutant strains ($\Delta vvhA$, $\Delta rtxA1$ and $\Delta vvhA \Delta rtxA1$) at a moi of 0.5. Haemolysis [percentage of lysed cells (% lysis)] and *vvhA*/*rtxA1* transcription [fold induction (FI) in artificial blood vs serum] were determined at 1, 3 and 6 h post-infection. Results are presented as average (\pm standard error) of three independent biological experiments. *Significant differences in % lysis between R99 and each mutant strain were determined using the unpaired Student's *t*-test ($p < 0.05$); # significant differences between *FlrtxA1* and *FlvvhA* were determined using the unpaired Student's *t*-test ($p < 0.05$).

A

Accession	SELECTED DEGs INVOLVED IN CAPSULE-LPS BIOSYNTHESIS	ES	HS+Fe	*Iron-stimulon	*Fur-regulon
Capsule biosynthesis					
WP_039448568.1	Glycosyltransferase SypJ	-	5.32	-	-
WP_039448561.1	Polysaccharide biosynthesis chain length regulator SypO	-2.94	-	-19.87	-51.54
WP_039448552.1	Glycosyltransferase SypP	-	3.33	-	-
WP_017422401.1	Capsular polysaccharide synthesis enzyme CpsD , exopolysaccharide synthesis	-	3.75	-	-
O-antigen biosynthesis					
WP_013571015.1	UDP-glucose 4-epimerase GalE	3.45	-3.86	-	-
WP_039449551.1	LipidA core-O-antigen ligase WaaL	2.44	-	4.12	3.29
WP_039450619.1	Low molecular weight protein-tyrosine-phosphatase Wzb	2.74	-	18.42	52.01
WP_039450616.1	Tyrosine-protein kinase Wzc	2.31	-	18.07	33.8
WP_039450678.1	dTDP-4-dehydrorhamnose reductase RfbD	2.28	-	21.43	4.01
WP_039450609.1	dTDP-4-dehydrorhamnose 3,5-epimerase RfbC	2.47	-	4.45	63.13
WP_011078757.1	UDP-N-acetylglucosamine 1-carboxyvinyltransferase murA	2.11	-2.24	25.36	29.51
NAN	Membrane protein involved in the export of O-antigen	2.11	-4.50	-	-
WP_088900111.1	O-antigen acetylase	-	10.22	-	6.5
WP_080540332.1	Lipopolysaccharide biosynthesis protein RffC	4.24	-2.02	15.65	18.24

B

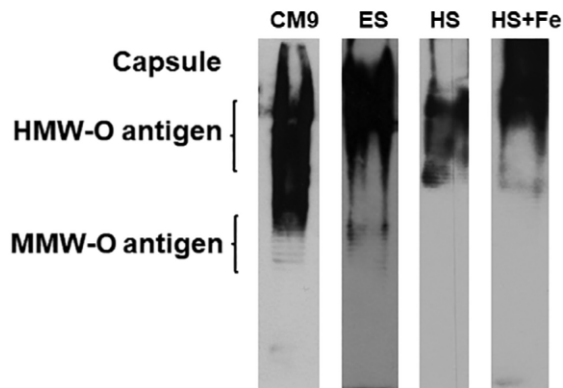


Fig. 3. LPS and capsule of *V. vulnificus* R99 strain in serum and the related-transcriptomic results. A. *Transcriptomic results.* Selection of differentially expressed genes in serum [eel serum (ES), human serum (HS) and iron-overloaded human serum (HS+Fe)] involved in capsule and LPS biosynthesis. Numbers represent fold-change values in ES (ES vs CM9), HS+Fe (HS+Fe vs CM9), *iron stimulon (CM9-Fe vs CM9 +Fe) (Pajuelo et al., 2016) and *Fur regulon (*Δfur* vs R99) (Pajuelo et al., 2016). NAN: gene with no accession number assigned. B. *LPS and capsule in serum.* Bacteria were grown for 6 h in CM9, ES, HS and HS+Fe. Then, cell-associated polysaccharides (LPS + capsule) were extracted with the method of Hitchcock and Brown (1983) and quantified using the Total Carbohydrate Assay Kit (BioVision). A 10 μg of cell-associated-polysaccharides were separated by SDS-PAGE on discontinuous gels (4% stacking gel, 10% separating gel), transferred to a PVDF membrane, subjected to immunoblot analysis with antibodies against cell-envelopes of R99 (diluted 1:3000) and developed following incubation with anti-rabbit IgG HRP-conjugated secondary antibody [diluted 1:10000 (Sigma)] using Immobilon Western Chemiluminescent HRP Substrate (Millipore). HMW, high molecular weight. MMW, medium molecular weight.

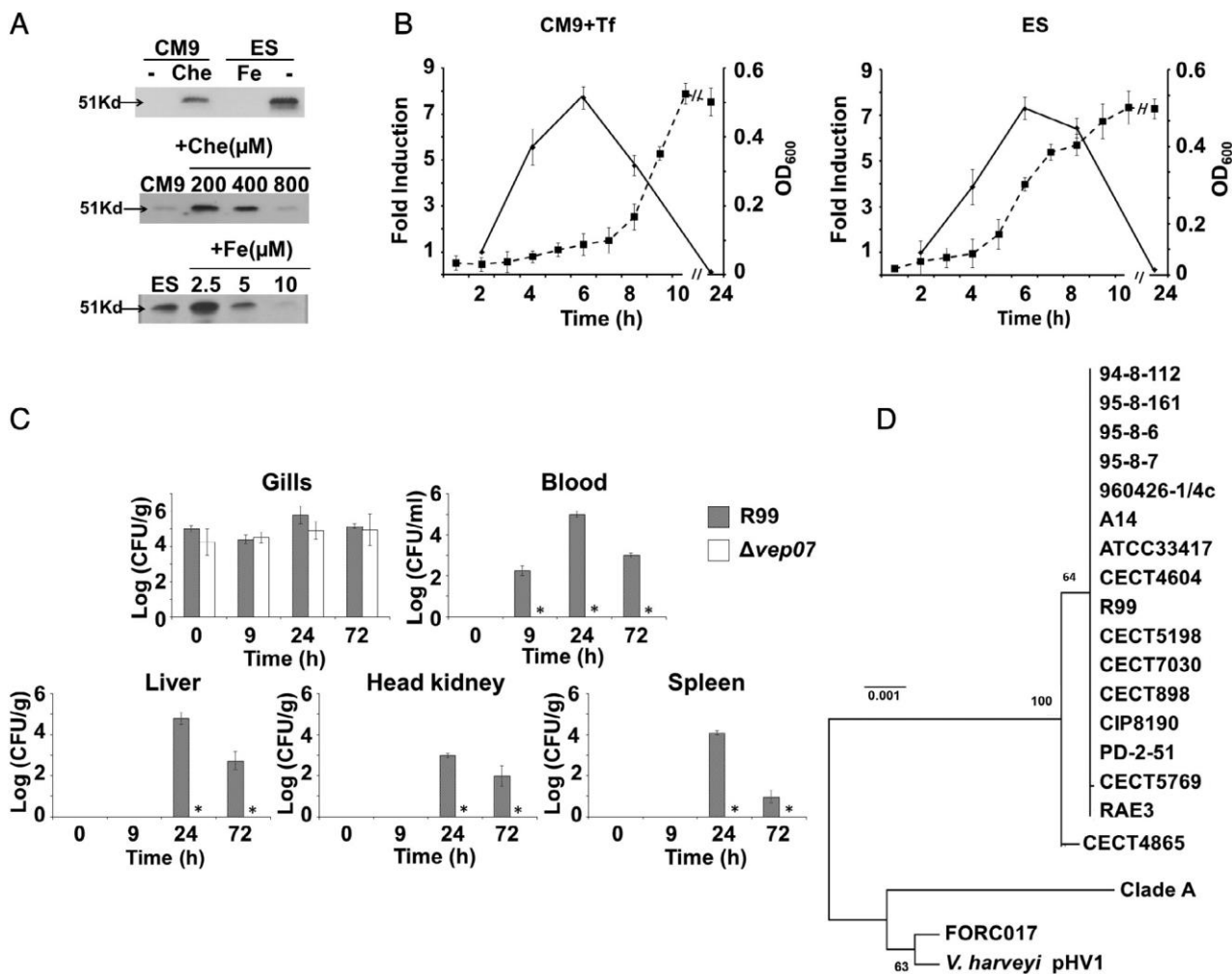


Fig. 4. *vep07*: protein characterization, transcription, role in virulence and phylogeny. A. *Translation vs iron concentration.* R99 was cultured in CM9 [without (-)] or with the iron-chelator 2,2'-bipyridyl (Che) or eel serum (ES) [without (-) or with added iron as FeCl₃ (Fe)] for 18 h. The cells were lysed, and 5 μ g of the insoluble protein fraction were separated by SDS-PAGE on discontinuous gels (4% stacking gel, 10% separating gel) and immunostained with anti-rVep07 serum. B. *Transcription vs growth.* *vep07* transcription levels (solid line) vs bacterial growth (dotted line) in CM9 supplemented with human transferrin 10 μ M (CM9 + Tf) or eel serum (ES). Each point represents the average of the fold induction (compared with CM9) or the OD₆₀₀ values of three independent biological samples (\pm standard error) that were statistically analysed using the unpaired Student's t-test ($p < 0.05$). C. *Eel colonization and invasion.* Groups of 24 eels per strain (three animals per sampling point) were infected by immersion with either the wild type or the mutant strain at the same dose (2×10^6 CFU ml⁻¹) and gills, blood, liver, head kidney and spleen were sampled for bacterial counting on TSA-1 (1% NaCl) at 0, 9, 24 and 72 h post-infection. Results are presented as average (\pm standard error) of three independent biological experiments (three sampled animals per experiment, sampling time and organ). *Significant differences between the R99 and *vep07* mutant strain ($p < 0.05$). D. *Phylogeny.* The evolutionary history was inferred by using the Maximum Likelihood method based on the Tamura 3-parameter model (Tamura, 1992). The initial tree(s) with the highest log likelihood (-2065.08) is shown. The percentage of the trees in which the associated taxa clustered together is shown next to the branches. The initial tree(s) for the heuristic search were obtained automatically by applying the Neighbour-Join and BioNJ algorithms to a matrix of pairwise distances estimated using the Maximum Composite Likelihood approach and then selecting the topology with the superior log likelihood value. The tree is drawn to scale, with branch lengths measured in the number of substitutions per site. The analysis involved 20 nucleotide sequences. All positions containing gaps and missing data were eliminated. There were a total of 1396 positions in the final dataset. The evolutionary analyses were conducted using MEGA7 (Kumar et al., 2016).

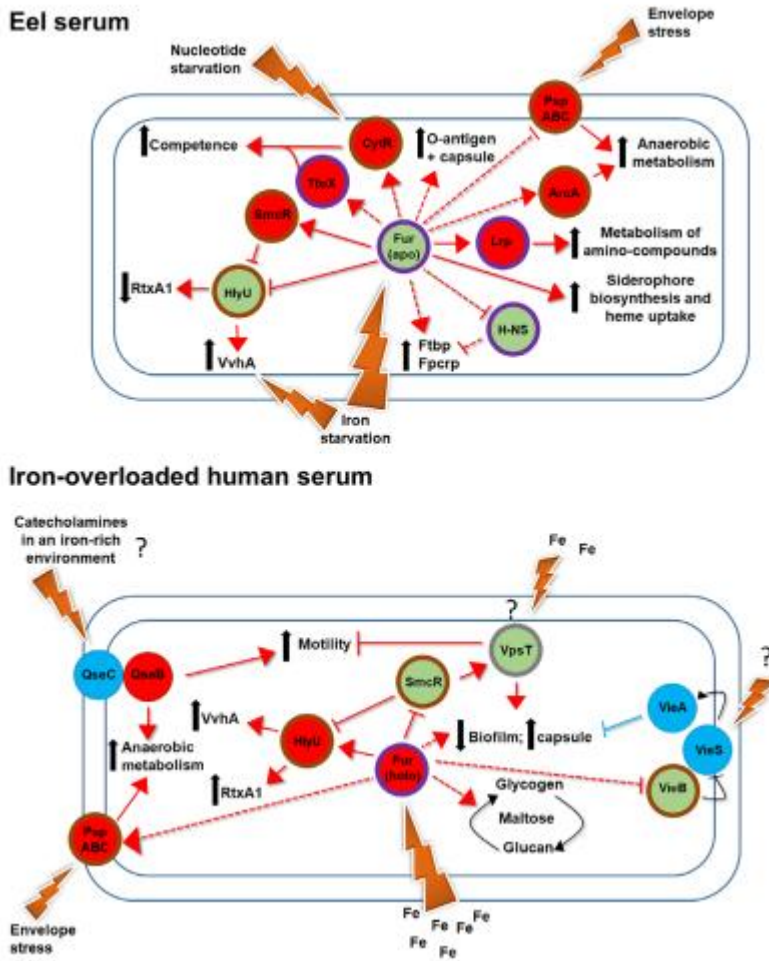
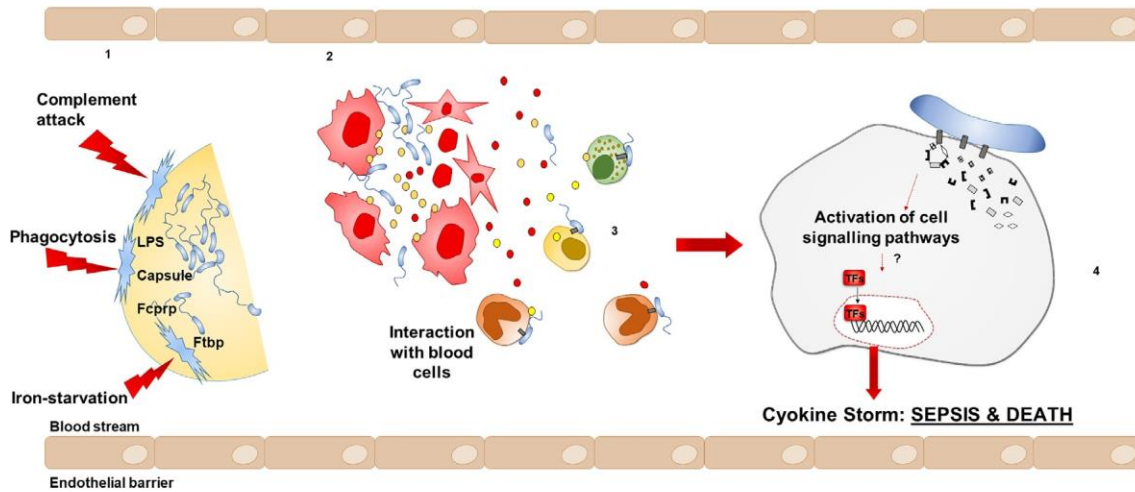


Fig. 5. Regulatory network, external stimulus and phenotype presented by zoonotic *V. vulnificus* growing in serum: a holistic model per susceptible host. The models show the main regulators and sensors that would respond to the putative external signals in the serum as well as the resultant phenotype. The models are based on our transcriptomic and phenotypic results as well as on data from the literature (Brinkman et al., 2003; Meibom et al., 2005; Krasteva et al., 2010; Shao et al., 2011; Antonova et al., 2012; Kim et al., 2013; Weigel et al., 2015; Pajuelo et al., 2016; Ho et al., 2017). The regulators and sensors are presented as bubbles in *red* (upregulated in our transcriptome), *green* (downregulated in our transcriptome) and *blue* (predicted according to the literature but not found in our transcriptome) surrounded by line *purple* [belongs to both iron stimulon and Fur regulon (Pajuelo et al., 2016)], *brown* [belongs to the Fur regulon (Pajuelo et al., 2016)] or *grey* [belongs to the iron stimulon (Pajuelo et al., 2016)]. Direct/indirect interaction between regulators and the predicted bacterial phenotype are shown as lines (confirmed results supported by this work and the literature) or dotted lines (proposed in this work but without previous evidences in the literature). See the full text for further information.

EEL BLOOD



IRON-OVERLOADED HUMAN BLOOD

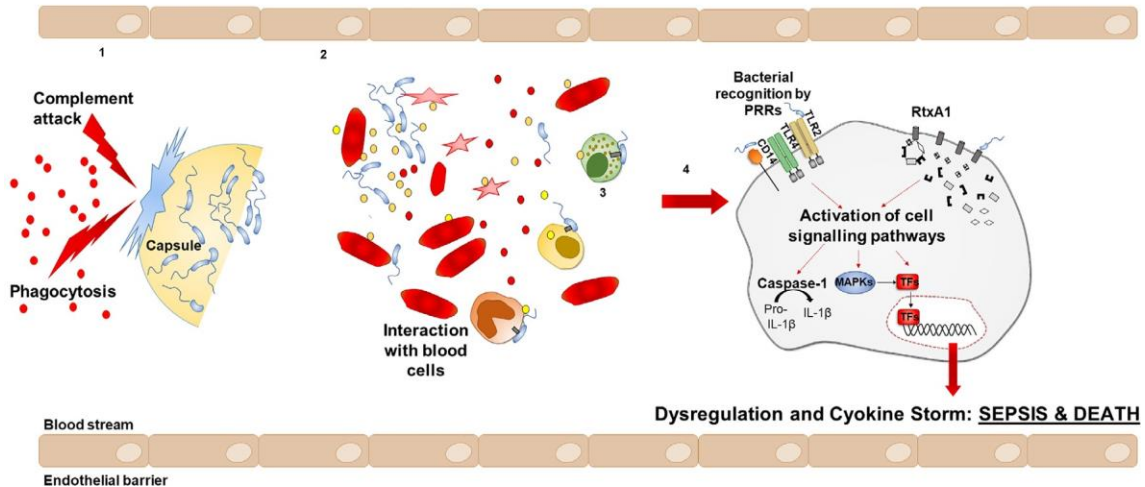


Fig. 6. Main virulence- and survival-related factors expressed by zoonotic *V. vulnificus* in host blood and their predicted function in septicemia. Model in eel. In eel blood, *V. vulnificus* cells detect iron starvation and express an adapted external envelope that contains two plasmid outer membrane proteins (OMPs), a receptor for eel transferrin (Ftbp) and a protective protein against eel complement and phagocytosis (Fcprp), embedded in an LPS enriched in the high/medium molecular weight part of the O-antigen and surrounded by a capsule (1). As a consequence, the bacteria resist in serum and multiply, secreting VvhA (yellow balls), a cytotoxin that lyses erythrocytes, which are very abundant in eel blood (approximately 10^9 cell ml^{-1}), which in turn, liberate haemoglobin creating a microenvironment rich in heme iron (2). In these conditions, and after contact with blood cells, the RtxA1 (in grey) is produced and secreted, entering into the eukaryotic cell (3) and causing a hypothetical cytokine storm, by unknown signalling cascades (4). Model in an iron-overloaded human. In the blood from a risk patient, the *V. vulnificus* cells detect iron excess (red balls) and express an adapted external envelope enriched in a capsule that protects them against both complement and phagocytosis (1). The protected bacteria multiply and produce both VvhA (yellow ball) and RtxA1 (grey bars), which collaborate in cellular destruction (3). When RtxA1 interacts with the appropriate immune cell, it triggers a cytokine storm by inducing the overexpression of inflammation mediators as described by Murciano et al. (2017) [Figure modified from the work of Murciano et al. (2017)]. Bacterial and eukaryotic cells are